

# Galactic dynamics in the presence of scalaron: A perspective from $f(R)$ gravity

Gayatri Mohan \* and Umananda Dev Goswami<sup>†</sup> <sup>‡</sup>  
Department of Physics, Dibrugarh University, Dibrugarh 786004, Assam, India

We consider  $f(R)$  modified gravity theory incorporating the chameleon mechanism to address galactic dynamics. By employing the metric formalism and utilizing a conformal transformation, we simplify the field equations and describe the extra degree of freedom  $f_R$  via a scalar field (scalaron) with chameleonic behavior. A recently proposed  $f(R)$  model is analyzed to illustrate this behavior effectively. Subsequently, the rotational velocity equation including the scalaron's contribution is derived for a test particle in a static, spherically symmetric spacetime. Then we generate rotation curves and fit them to observational data of thirty seven galaxies using two fitting parameters,  $M_0$  and  $r_c$ , the total mass and core radius of a galaxy respectively.

Keywords: Modified gravity theory; Chameleon mechanism; Scalaron; Conformal transformation; Rotation curves.

## I. INTRODUCTION

The captivating enigma of dark matter (DM) and the accelerated expansion of the Universe are two formidable challenges of modern astrophysics and cosmology. Behaviors of observed galactic rotation curves [1–3] and gravitational lensing [4, 5] in galaxies and their clusters manifest the mass discrepancy in them and suggest the need for DM as a major matter component in the Universe. However, there is currently no experimental evidence supporting the existence of this elusive missing matter and dark energy responsible for late-time acceleration. These two so-called greatest puzzles of modern times have stimulated the scientific community to think about the modifications of Einstein's theory of General relativity (GR) and upshot the modified theories of gravity (MTGs) [6–12]. These theories are the consequences of the modification of gravity part of Einstein-Hilbert (EH) action and can be treated as a modified approach for explaining the issues of DM [13–21] as well as dark energy (DE), the dominant unknown component of mass-energy that is supposed to be responsible for the present accelerated expansion of the Universe [22–25].  $f(R)$  gravity [26–29],  $f(R, T)$  gravity [9, 30, 31], Gauss-Bonnet gravity [32, 33], Scalar-tensor theories [34, 35], Braneworld models [36] etc. are some widely studied gravity theories as alternatives to GR. Among different MTGs, the simplest modification of GR is the  $f(R)$  theory of gravity, proposed by H. A. Buchdahl in 1970 through the replacement of the Ricci scalar  $R$  in the EH action with an arbitrary function  $f(R)$  of it [26]. In this theory, field equations can be derived from the action using mainly two approaches: one is the metric formalism in which the affine connection  $\Gamma_{\alpha\beta}^{\rho}$  depends on the metric  $g_{\mu\nu}$  and the field equations are obtained by varying the action with respect to the metric only. Another is the Palatini formalism in which the field equations are derived from the variation of the action treating affine connection and the metric as independent variables [37]. Such covariant modifications of GR always introduce an extra degree of freedom besides the tensor degree of freedom. We restrict ourselves to metric  $f(R)$  theory in this work. This theory can be reformulated as a scalar-tensor theory by describing this additional degree of freedom as a scalar field called scalaron [38]. Indeed, it is equivalent to a scalar-tensor theory if it is transformed to the Einstein frame via conformal transformation [39–45]. Under this transformation the scalaron field couples with matter minimally and acquires effective mass that depends sensitively on the density of the environment. The scalaron field exhibiting such a local matter density dependent physical property is referred to as a chameleon field and the mechanism involved is called the chameleon mechanism [46, 47]. It is a screening mechanism in which the scalaron changes its properties to fit the surroundings where the field is allowed to exhibit significant mass in dense environments, such as within the solar system, and less mass in low density regions, such as on cosmological scales. In high density surroundings, the force induced by the scalaron field is suppressed while in low density localities it mediates a force of gravitational strength extending its impacts over a long range [48, 49]. Such a low-mass scalar field may be a genuine substitute for DM.

A range of studies have been undertaken to investigate the scalaron as an alternative to DM and DE in MTGs. Especially, the effectiveness of chameleonic viable  $f(R)$  models in mimicking the DM component of the Universe

---

<sup>†</sup> Corresponding author

\*Email: [gayatrimohan704@gmail.com](mailto:gayatrimohan704@gmail.com)

<sup>‡</sup>Email: [umananda2@gmail.com](mailto:umananda2@gmail.com)

was explored at different scales. Ref. [50] has explained the DM problem in chameleon  $f(R)$  gravity by considering a model of the form  $f(R) = R^{(1+\delta)}/R_c^\delta$  and suggested that behaviour of the scalaron derived from this model makes it suitable to mimic as DM. The study of DM taking into account the screening mechanism in the Starobinsky model is addressed in Ref. [51]. This study has analysed three different possible ways for revealing light scalaron to be a DM candidate and also estimated its lifetime by investigating the coupling between the scalaron and standard model particles. Refs. [19, 52] have illustrated DM based on chameleonic features of scalaron. It is suggested in Ref. [19] that the mass of the scalaron can be found to be close to the mass of ultralight axions so that it can mimic DM candidate. Refs. [53] investigated the effects of a chameleon scalar field on rotation curves of certain late-type low surface brightness (LSB) galaxies and observed a cuspiest rotation curve for each galaxy. Some other investigations [54–58] have been conducted by analyzing the chameleon scalar field to address DM issues. In addition to the dark matter and dark energy issues, multiple investigations such as exploration of black hole properties [59], determination of the gravitational wave echo frequencies emitted by ultra-compact objects like strange stars [60] etc. have been performed in  $f(R)$  gravity that will enable to test the predictions of this theory with observations. These works have motivated us to consider a study for the explanation of this exotic matter component by exploring the chameleonic behaviour of a recently introduced  $f(R)$  gravity model [28, 61]. Specifically, in this study, we intend to check the chameleonic viability of this model of  $f(R)$  gravity by examining the characteristics of its scalar degree of freedom (scalaron) as no chameleonic study has been performed with this specific model till now. The principal focus of this work is to investigate the impact of scalaron on galactic dynamics taking into consideration of chameleon mechanism via conformal transformation in metric  $f(R)$  gravity theory, utilizing this new model within this gravitational theory. With this objective, we first present field equations of metric  $f(R)$  gravity. Then by conformal transformation, the fourth-order equations generated by the theory are simplified to second-order equations through the introduction of a scalar field that shows chameleonic features. We study this feature of the field shown by the model with a correction of the singularity problem usually suffered by  $f(R)$  gravity models [19]. The singularity correction makes scalaron reasonably light in denser regions, such as in the galactic center, which may mitigate the suppression of the field due to its induced force. Using the singularity corrected model, we obtain rotational velocity with scalaron contribution term for test particles moving around galaxies in stable circular orbits. The rotation curves thus predicted by the theory are then fitted with observations of some samples of high surface brightness (HSB), LSB and dwarf galaxies, and achieve well-fitted rotation curves almost for all sample galaxies.

The work is organized as follows. In Section II, we present the field equations of the  $f(R)$  gravity and then via conformal transformation the minimal coupling of a scalar field (scalaron) to non-relativistic matter is presented. Also, the equation of motion of the scalaron, its effective potential and expression for mass are derived. In Section III, by considering a new  $f(R)$  gravity model [28, 61] as mentioned above, the chameleonic behavior of the scalaron is outlined. In Section IV, assuming a static, spherically symmetric spacetime the orbital motion of a test particle in the presence of the scalaron is presented. Finally, we conclude our work in Section V with some future prospects. In this work, we set  $c = \hbar = 1$  and adopt the metric signature as  $(-, +, +, +)$ .

## II. $f(R)$ GRAVITY FIELD EQUATIONS AND CONFORMAL TRANSFORMATION

### A. Field equations in metric formalism

To derive field equations in metric formalism, we proceed from the action of  $f(R)$  gravity, which is given as [37, 62]

$$S = \frac{1}{2\kappa^2} \int d^4x \sqrt{-g} f(R) + S_m(g_{\mu\nu}, \psi), \quad (1)$$

where  $g$  is the determinant of the metric  $g_{\mu\nu}$ ,  $\kappa^2 = 8\pi G = M_{pl}^{-2}$ ,  $M_{pl}$  is the reduced Plank mass  $\approx 2.4 \times 10^{18}$  GeV, and  $S_m(g_{\mu\nu}, \psi) = \int d^4x \sqrt{-g} \mathcal{L}_m(g_{\mu\nu}, \psi)$  is the matter action with the non-relativistic matter field  $\psi$ . The Ricci scalar  $R$  is defined as  $R = g^{\mu\nu} R_{\mu\nu}$ , where the Ricci tensor  $R_{\mu\nu}$  is expressed in the form:

$$R_{\mu\nu} = R_{\mu\sigma\nu}^\sigma = \partial_\sigma \Gamma_{\mu\nu}^\sigma - \partial_\nu \Gamma_{\mu\sigma}^\sigma + \Gamma_{\mu\nu}^\lambda \Gamma_{\lambda\sigma}^\sigma - \Gamma_{\mu\sigma}^\lambda \Gamma_{\lambda\nu}^\sigma. \quad (2)$$

The variation of action (1) with respect to metric  $g_{\mu\nu}$  results in the field equations of the metric formalism of  $f(R)$  gravity as given by

$$f_R R_{\mu\nu} - \frac{1}{2} g_{\mu\nu} f(R) - [\nabla_\mu \nabla_\nu - g_{\mu\nu} \square] f_R = \kappa^2 T_{\mu\nu}(g_{\mu\nu}, \psi). \quad (3)$$

Here,  $f_R = df/dR$ ,  $\nabla_\mu$  is the covariant derivative connected with the Levi-Civita connection of metric  $g_{\mu\nu}$ ,  $\square = \nabla^\mu \nabla_\mu$  is the Laplace operator in four dimensions and  $T_{\mu\nu}$  is the energy-momentum tensor which satisfies the condition:

$\nabla^\mu T_{\mu\nu} = 0$ , and usually it is given by

$$T_{\mu\nu} = -\frac{2}{\sqrt{-g}} \frac{\delta S_m(g_{\mu\nu}, \psi)}{\delta g^{\mu\nu}} \equiv -\frac{2}{\sqrt{-g}} \frac{\delta(\sqrt{-g} \mathcal{L}_m(g_{\mu\nu}, \psi))}{\delta g^{\mu\nu}}. \quad (4)$$

The field equations (3) in the form of Einstein field equations can be written as

$$G_{\mu\nu} = \frac{\kappa^2 T_{\mu\nu}}{f_R} + g_{\mu\nu} \frac{f(R) - Rf_R}{2f_R} + \frac{\nabla_\mu \nabla_\nu f_R - g_{\mu\nu} \square f_R}{f_R} = \frac{\kappa^2}{f_R} (T_{\mu\nu} + T_{\mu\nu}^{eff}), \quad (5)$$

where  $T_{\mu\nu}^{eff}$  is the effective energy-momentum tensor of the following form:

$$T_{\mu\nu}^{eff} = \frac{1}{\kappa^2} \left[ g_{\mu\nu} \frac{f(R) - Rf_R}{2} + (\nabla_\mu \nabla_\nu - g_{\mu\nu} \square) f_R \right]. \quad (6)$$

Further, the modified field equations (5) may also take the form:

$$f_R [G_{\mu\nu} + G_{\mu\nu}^d] = \kappa^2 T_{\mu\nu}, \quad (7)$$

where

$$G_{\mu\nu}^d = \frac{1}{f_R} \left[ g_{\mu\nu} \frac{Rf_R - f(R)}{2} - (\nabla_\mu \nabla_\nu - g_{\mu\nu} \square) f_R \right].$$

is the deviated part of the Einstein tensor that appears due to the change in the curvature introduced by the  $f(R)$  gravity. The effective energy-momentum tensor is also emerged due to the same reason, i.e. the change of the behavior of curvature in  $f(R)$  gravity.

The existence of the last two terms on the left hand side of equations (3) expresses them as fourth-order partial differential equations. The trace of equations (3) is obtained as

$$3\square f_R + f_R R - 2f(R) = \kappa^2 T, \quad (8)$$

where  $T = T_\mu^\mu$  is the trace of the energy-momentum tensor and  $\square f_R = \partial_\mu (\sqrt{-g} g^{\mu\nu} \partial_\nu f_R) / \sqrt{-g}$ . Equation (8) is the equation of motion for  $f_R$  that determines the dynamics of  $f_R$ . It shows that the Ricci scalar  $R$  is dynamic. With  $f(R)$  as a linear function of  $R$ ,  $f_R$  is constant and hence  $\square f_R = 0$ . In this case, the theory reduces to GR leading the equation (8) as  $R = -\kappa^2 T$ , implying the direct dependence of Ricci scalar on matter. Instead, in  $f(R)$  theory  $\square f_R$  does not vanish. It signifies that the theory includes an extra propagating degree of freedom  $f_R$ , called the scalar degree of freedom that characterizes the modification of gravity and plays a central role in explaining the galactic dynamics without dark matter [50, 51, 63]. With this conformity, we proceed with the conformal transformation in the following subsection to identify  $f_R$  conveniently in an explicit form.

## B. Conformal transformation

Conformal transformation is a mathematical technique used expediently to simplify the equations of motion in the Jordan frame into an amenable form [64]. In fact, it is a tool that physicists generally use for a better understanding of the implications of MTGs and their connection to the standard framework of GR. Through a conformal transformation, the higher-order and non-minimally coupled terms can always be shown as the sum of the Einstein gravity and one or more minimally coupled scalar field(s) [11]. In the case of the fourth-order gravity when undergoing this transformation, gives one scalar field with the Einstein gravity. Before performing such a transformation we recast the action (1) in the following form [37]:

$$S = \int d^4x \sqrt{-g} \left[ \frac{Rf_R}{2\kappa^2} - X(R) \right] + \int d^4x \sqrt{-g} \mathcal{L}_m(g_{\mu\nu}, \psi), \quad (9)$$

where

$$X(R) = \frac{1}{2\kappa^2} [Rf_R - f(R)]. \quad (10)$$

Equation (10) can be treated as the potential of an auxiliary scalar field defined in the Jordan frame [19, 62, 65]. This potential is non-zero only when  $f_R \neq \text{constant}$ . In the case  $f(R) = R$ , it becomes zero and hence the theory reduces to

GR. We consider now the following conformal transformation that reduces the fourth-order non-minimally coupled field equations (3) into a minimally coupled tractable form through the transition of the Jordan frame metric  $g_{\mu\nu}$  to the Einstein frame metric  $\tilde{g}_{\mu\nu}$  as [37, 66–68]

$$g_{\mu\nu} \rightarrow \tilde{g}_{\mu\nu} = \Omega^2 g_{\mu\nu}, \quad (11)$$

where  $\Omega^2$  is a non-vanishing regular function called the conformal factor. Under transformation rule (11) the Ricci scalars  $R$  and  $\tilde{R}$  in these two respective frames are related by

$$R = \Omega^2 \left[ \tilde{R} + 6 \square (\ln \Omega) - 6 \tilde{g}^{\mu\nu} \nabla_\mu (\ln \Omega) \nabla_\nu (\ln \Omega) \right]. \quad (12)$$

Also, the determinants of the metric tensors in the two frames hold the following relation:

$$\sqrt{-g} = \Omega^{-4} \sqrt{-\tilde{g}}. \quad (13)$$

Using equations (9), (12) and (13), and also Gauss's theorem the action in Einstein's frame is derived as given below:

$$S_E = \int d^4x \sqrt{-\tilde{g}} \left[ \frac{1}{2\kappa^2} f_R \Omega^{-2} \{ \tilde{R} - 6 \tilde{g}^{\mu\nu} \nabla_\mu (\ln \Omega) \nabla_\nu (\ln \Omega) \} - \frac{X(f_R)}{\Omega^4} \right] + \int d^4x \Omega^{-4} \sqrt{-\tilde{g}} \mathcal{L}_m (\Omega^{-2} \tilde{g}_{\mu\nu}, \psi). \quad (14)$$

At this stage, we are in a position to introduce a new scalar field called scalaron  $\phi$  defined by [69]

$$\phi = \frac{1}{\kappa} \sqrt{\frac{3}{2}} \ln f_R. \quad (15)$$

This field corresponds to an extra scalar degree of freedom  $f_R$  in  $f(R)$  theory as

$$f_R = e^{\sqrt{\frac{2}{3}} \kappa \phi}. \quad (16)$$

Using the scalar field defined in equation (15) and choosing the conformal factor  $\Omega^2 = f_R$ , the action (14) in Einstein's frame can be written in the form:

$$S_E = \frac{1}{2\kappa^2} \int d^4x \sqrt{-\tilde{g}} \tilde{R} + \int d^4x \sqrt{-\tilde{g}} \left[ -\frac{1}{2} \tilde{g}^{\mu\nu} \partial_\mu \phi \partial_\nu \phi - V(\phi) \right] + \int d^4x \frac{\sqrt{-\tilde{g}}}{f_R^2} \mathcal{L}_m (f_R(\phi)^{-1} \tilde{g}_{\mu\nu}, \psi). \quad (17)$$

Here, we may write  $f_R(\phi)^{-1} = e^{2\beta\kappa\phi}$  which gives constant coupling factor  $\beta = -1/\sqrt{6}$ . It indicates that the scalar field is directly coupled to matter field  $\psi$  with a constant coupling  $\beta$  in the Einstein frame. Further,  $V(\phi)$  represents the potential of the scalaron field defined by

$$V(\phi) = \frac{X}{f_R^2} = \frac{1}{2\kappa^2} \left[ \frac{Rf_R - f(R)}{f_R^2} \right]. \quad (18)$$

Equation (17) shows that  $f(R)$  gravity can be expressed by means of GR along with the additional scalar field, the scalaron, that holds noteworthy significance in the theory.

### C. Equation of motion of scalaron and its mass

Variation of action (17) with respect to  $\phi$  gives the following equation:

$$\tilde{\square} \phi - \frac{dV(\phi)}{d\phi} + \frac{1}{\sqrt{-\tilde{g}}} \frac{\partial(\sqrt{-\tilde{g}} \mathcal{L}_m)}{\partial \phi} = 0, \quad (19)$$

where

$$\tilde{\square} = \frac{1}{\sqrt{-\tilde{g}}} \partial_\mu (\sqrt{-\tilde{g}} \tilde{g}^{\mu\nu} \partial_\nu).$$

Again, the derivative factor of the last term on the left-hand side of equation (19) can be expressed as

$$\frac{\partial(\sqrt{-g} \mathcal{L}_m)}{\partial\phi} = -\frac{\sqrt{-g}}{2} \left( -\frac{2}{\sqrt{-g}} \frac{\delta(\sqrt{-g} \mathcal{L}_m)}{\delta g^{\mu\nu}} \right) \frac{\partial g^{\mu\nu}}{\partial\phi} = -\frac{\sqrt{-g}}{2} T_{\mu\nu} \frac{\partial g^{\mu\nu}}{\partial\phi}. \quad (20)$$

Also we have,

$$\tilde{T}_{\mu\nu} = -\frac{2}{\sqrt{-\tilde{g}}} \frac{\delta(\sqrt{-g} \mathcal{L}_m)}{\delta \tilde{g}^{\mu\nu}} = \frac{T_{\mu\nu}}{f_R}. \quad (21)$$

Use of equations (11) in contravariant form, and equations (13) and (21) in equation (20) yields

$$\frac{\partial(\sqrt{-g} \mathcal{L}_m)}{\partial\phi} = -\frac{\sqrt{-\tilde{g}}}{2f_R} \frac{df_R}{d\phi} \tilde{T}^\mu{}_\mu. \quad (22)$$

From  $\tilde{T}^\mu{}_\mu = T^\mu{}_\mu / f_R^2$ , the relation between the trace of the energy-momentum tensors in two frames and equation (22) together with relation (16) we can rewrite scalaron's equation of motion (19) as

$$\tilde{\square} \phi - \frac{dV_{eff}}{d\phi} = 0, \quad (23)$$

where

$$\begin{aligned} \frac{dV_{eff}(\phi)}{d\phi} &= \frac{dV(\phi)}{d\phi} + \frac{\kappa}{\sqrt{6}} \tilde{T}^\mu{}_\mu \\ &= \frac{dV(\phi)}{d\phi} + \frac{\kappa}{\sqrt{6}} e^{-2\sqrt{\frac{2}{3}}\kappa\phi} T^\mu{}_\mu. \end{aligned} \quad (24)$$

$V_{eff}(\phi)$  refers the effective potential of the scalaron field. Equation (23) shows in conjunction with equation (24) that scalaron couples to the matter field in the Einstein frame with a constant coupling strength  $1/\sqrt{6}$  as mentioned earlier. In the Jordan frame, this coupling strength decreases exponentially with the increasing scalaron field value. Also it should be noted that as matter moves on geodesic of Jordan frame metric, the Einstein frame energy-momentum tensor  $\tilde{T}_{\mu\nu}$  is not covariantly conserved, i.e.  $\tilde{\nabla}_\mu \tilde{T}_{\mu\nu} \neq 0$  [44]. By integrating equation (24) one may obtain the effective potential  $V_{eff}$  of the scalaron as follows:

$$V_{eff} = V(\phi) - \frac{1}{4} e^{-2\sqrt{\frac{2}{3}}\kappa\phi} T^\mu{}_\mu. \quad (25)$$

The presence of the second term in equation (25) indicates that the dynamics of the scalaron described by the equation (23) is influenced by the surrounding matter content represented by  $T^\mu{}_\mu$ . Consequently, the effective potential results in the environment matter dependent scalaron mass  $m_\phi$  as the square of  $m_\phi$  corresponds to the second order derivative of effective potential at the minimum of the field value  $\phi_0$ . So, we obtain the mass of the scalaron by differentiating equation (24) with respect to  $\phi$  at  $\phi = \phi_0$  as

$$m_\phi^2 = \frac{d^2 V_{eff}(\phi)}{d\phi^2} = \frac{d^2 V(\phi_0)}{d\phi^2} - \frac{2\kappa^2}{3} e^{-2\sqrt{\frac{2}{3}}\kappa\phi_0} T^\mu{}_\mu. \quad (26)$$

From equation (26) it is found that the potential  $V(\phi)$  is not only the determining factor of the scalaron mass, it is strongly affected by  $T^\mu{}_\mu$  of environment as mentioned above. To explicitly express the factor contributed by the potential  $V(\phi)$  to the scalaron mass and also to express the scalaron mass in a suitable form we proceed as follows. From equations (15) and (18) we may write,

$$\frac{dV(\phi)}{dR} = \frac{1}{2\kappa^2} \frac{2f(R)f_{RR} - Rf_R f_{RR}}{f_R^3}. \quad (27)$$

$$\frac{d\phi}{dR} = \frac{1}{\kappa} \sqrt{\frac{3}{2}} \frac{f_{RR}}{f_R}. \quad (28)$$

These two equations provide us the derivatives of  $V(\phi)$  with respect to  $\phi$  as

$$\frac{dV(\phi)}{d\phi} = \frac{1}{\sqrt{6}\kappa} \frac{2f(R) - Rf_R}{f_R^2}. \quad (29)$$

From this equation, we may obtain,

$$\frac{d^2V(\phi)}{d\phi^2} = \frac{1}{3f_{RR}} \left[ 1 + \frac{Rf_{RR}}{f_R} - \frac{4f(R)f_{RR}}{f_R^2} \right]. \quad (30)$$

It should be mentioned that at the minimum of the scalaron field value i.e., at  $\phi = \phi_0$ , the effective potential satisfies the condition  $dV_{eff}(\phi_0)/d\phi = 0$ , which turns the left-hand side of equation (24) to zero. Thus, inserting equations (15) and (29) into (24), the stationary condition satisfied by the minimum of potential is obtained as

$$2f(R_0) - R_0 f_R(R_0) = -\kappa^2 T_\mu^\mu, \quad (31)$$

where  $R_0$  is the Ricci scalar corresponding to the minimum of the scalaron  $\phi_0$ . Using equations (30) and (31) we can write a general expression from equation (26) for  $m_\phi^2$  at minimum field value in the form given below:

$$m_\phi^2 = \frac{1}{3f_{RR}(R_0)} \left[ 1 - \frac{R_0 f_{RR}(R_0)}{f_R(R_0)} \right]. \quad (32)$$

This equation is useful to study scalaron mass for a specific  $f(R)$  gravity model.

### III. CHAMELEON MECHANISM IN A NEW $f(R)$ GRAVITY MODEL

In this section, we study the scalaron mass and its chameleonic behavior in a model specific case considering a recently proposed  $f(R)$  gravity model [28, 61], which is given by

$$f(R) = R - \frac{\alpha}{\pi} R_c \cot^{-1} \left( \frac{R_c^2}{R^2} \right) - \beta R_c \left[ 1 - e^{-\frac{R}{R_c}} \right], \quad (33)$$

where  $\alpha, \beta$  are two dimensionless positive constants and  $R_c$  is a characteristic curvature constant having the dimension same as the curvature scalar. For this model (33),  $f_R$  can be obtained as

$$f_R(R) = 1 - \frac{2\alpha R_c^3}{\pi R^3 \left( 1 + \frac{R_c^4}{R^4} \right)} - \beta e^{-\frac{R}{R_c}}. \quad (34)$$

Notably, in  $f(R)$  gravity, the curvature  $R$  and the trace of the energy-momentum tensor  $T_\mu^\mu$  are related through the modified trace equation (8), which shows how the function  $f(R)$  governs the spacetime curvature response in the presence of matter and energy. Here, we assume a large curvature limit, i.e.  $R \gg R_c$ , we can approximate equation (33) in this limit as

$$f(R) = R - \frac{\alpha R_c}{2} - \beta R_c. \quad (35)$$

Similarly, under this consideration equation (34) reduces to

$$f_R(R) = 1 - \frac{2\alpha R_c^3}{\pi R^3} - \beta e^{-\frac{R}{R_c}}. \quad (36)$$

The derivative of it appears as

$$f_{RR}(R) = \frac{6\alpha R_c^3}{\pi R^4} + \frac{\beta}{R_c} e^{-\frac{R}{R_c}}. \quad (37)$$

Assuming the energy-momentum tensor for an ideal non-relativistic matter we obtain  $T_\mu^\mu = -\rho$ , where  $\rho$  is the local matter energy density. Thus equation (31) which is a consequence of minimum effective potential ensues a relation between matter density and curvature in high curvature limit  $R \gg R_c$  as [19, 52]

$$R_0 = \rho\kappa^2 + \alpha R_c + 2\beta R_c. \quad (38)$$

This relation when used in equation (32), along with equations (36) and (37) for the respective  $f_R(R_0)$  and  $f_{RR}(R_0)$  terms, we obtain a local matter density dependent mass of the scalaron for the chosen model as

$$m_\phi^2 = \frac{\pi (\rho\kappa^2 + \alpha R_c + 2\beta R_c)^4}{3} \left[ \frac{R_c}{6\alpha R_c^4 + \pi\beta (\rho\kappa^2 + \alpha R_c + 2\beta R_c)^4 e^{-\frac{R_0}{R_c}}} - \frac{1}{\pi (\rho\kappa^2 + \alpha R_c + 2\beta R_c)^3 [1 - \beta e^{-\frac{R_0}{R_c}}] - 2\alpha R_c^3} \right]. \quad (39)$$

It is clear from equation (39) that the scalaron mass depends on matter density  $\rho$  of the surrounding environment and it increases as a certain power function of density  $\rho$ . This behaviour of the scalaron mass with increasing  $\rho$  confirms the chameleonic nature of the scalaron in the model we have considered for our study. We depict this particular behavior of scalaron mass in Fig. 1 for different values of model parameters by setting the characteristic curvature constant  $R_c = 1$  [28]. Of course there is no specific reason for choosing these particular values of model parameters. These are considered arbitrarily to study the variation of scalaron mass  $m_\phi$  with environment density. However, it is seen that for each set of parameters  $\alpha$  and  $\beta$ , the scalaron mass increases as the matter density increases. The plot in the left panel illustrates the variation of  $m_\phi$  for changing  $\beta$ , while the right panel demonstrates the effect of varying  $\alpha$  on  $m_\phi$ .

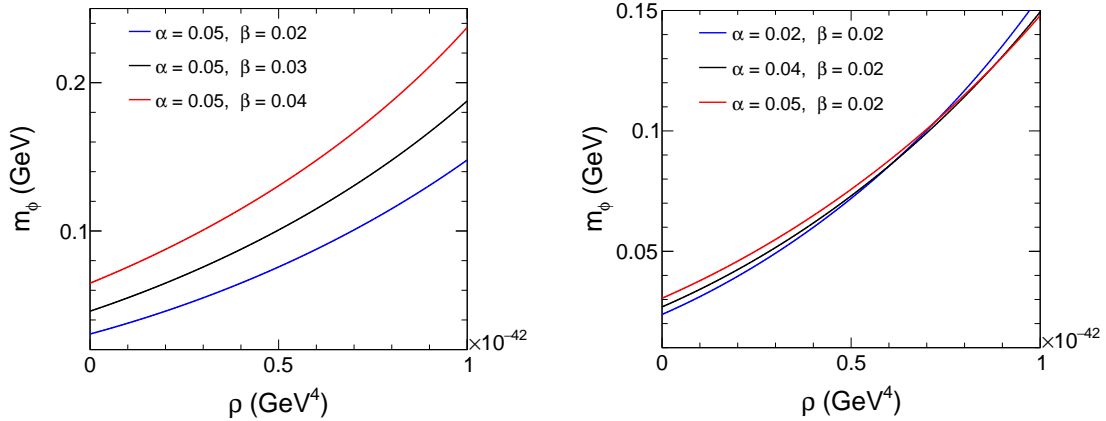


FIG. 1: Relations between scalaron mass and matter density for two sets of model parameters  $\alpha$  and  $\beta$  with  $R_c = 1$ . The left plot is for different values of  $\beta$  by fixing  $\alpha$  to 0.05 and the right plot is for different values of  $\alpha$  by fixing  $\beta$  to a value 0.02.

It is seen from equations (18) and (33) that the scalaron potential is a function of curvature scalar  $R$ . By substituting equation (16) into equation (18), it can also be expressed as a function of the scalaron field  $\phi$  where the relation between curvature scalar and scalaron field is given by [19, 52]

$$R = \left(\frac{2\alpha}{\pi}\right)^{1/3} R_c \left(1 - e^{\sqrt{\frac{2}{3}}\kappa\phi}\right)^{-1/3}, \quad (40)$$

which is obtained from equations (16) and (36) in high curvature regime approximation consideration. Although, the approximation made here is a bit stringent, the result gives us a clear indication of the presence of curvature singularity [70] which is discussed in Appendix A.

## IV. ROTATION CURVES AND SCALARON

### A. Galactic rotational velocity

To derive the equation of motion of a test particle (a star) using conformal coupling we consider the motion of the particle in a static gravitational field within a constant velocity region described by the following spherically symmetric metric:

$$ds^2 = -e^\mu dt^2 + e^\nu dr^2 + r^2 d\theta^2 + r^2 \sin^2 \theta d\varphi^2, \quad (41)$$

where the metric components  $\mu$  and  $\nu$  are functions of the radial coordinate  $r$  only. Since the conformal coupling given by equation (11) with the conformal factor expressed by equation (16) makes the interaction between scalaron field with matter distribution, we will use this coupling in the geodesic equation of the particle. On the other hand, the matter field  $\psi$  couples to Jordan frame metric  $g_{\mu\nu}$  instead of Einstein frame metric  $\tilde{g}_{\mu\nu}$  [44]. Hence the particle follows timelike geodesic of  $g_{\mu\nu}$  not that of  $\tilde{g}_{\mu\nu}$ . The geodesic of the particle is, therefore, given by the following equation [31, 71, 72]:

$$\frac{d^2 x^\eta}{d\tau^2} + \Gamma_{\mu\nu}^\eta \frac{dx^\mu}{d\tau} \frac{dx^\nu}{d\tau} = 0, \quad (42)$$

where the Christoffel symbol (connection coefficient) which governs the motion is defined as

$$\Gamma_{\mu\nu}^{\eta} = \frac{1}{2} g^{\eta\lambda} \left[ \frac{\partial g_{\mu\lambda}}{\partial x^{\nu}} + \frac{\partial g_{\nu\lambda}}{\partial x^{\mu}} - \frac{\partial g_{\mu\nu}}{\partial x^{\lambda}} \right]. \quad (43)$$

From equations (11) and (16), we have

$$g_{\mu\nu} = e^{-\sqrt{\frac{2}{3}}\kappa\phi} \tilde{g}_{\mu\nu}, \quad g^{\mu\nu} = e^{\sqrt{\frac{2}{3}}\kappa\phi} \tilde{g}^{\mu\nu}. \quad (44)$$

Each term of the right-hand side of equation (43) can be replaced by respective conformally transformed equations that are obtained from equation (44). Thus, a relation between the connection coefficients in the Jordan and the Einstein frames is established [72] which may be written as

$$\Gamma_{\mu\nu}^{\eta} = \tilde{\Gamma}_{\mu\nu}^{\eta} - \frac{\kappa}{\sqrt{6}} \left[ \frac{\partial\phi}{\partial x^{\nu}} \delta_{\mu}^{\eta} + \frac{\partial\phi}{\partial x^{\mu}} \delta_{\nu}^{\eta} - \frac{\partial\phi}{\partial x^{\lambda}} \tilde{g}^{\eta\lambda} \tilde{g}_{\mu\nu} \right]. \quad (45)$$

Substitution of this equation in equation (43) yields

$$\frac{d^2 x^{\eta}}{d\tau^2} + \tilde{\Gamma}_{\mu\nu}^{\eta} \frac{dx^{\mu}}{d\tau} \frac{dx^{\nu}}{d\tau} - \frac{\kappa}{\sqrt{6}} \left[ 2 \frac{\partial\phi}{\partial x^{\mu}} \frac{dx^{\mu}}{d\tau} \frac{dx^{\eta}}{d\tau} - \tilde{g}^{\eta\lambda} \frac{\partial\phi}{\partial x^{\lambda}} \tilde{g}_{\mu\nu} \frac{dx^{\mu}}{d\tau} \frac{dx^{\nu}}{d\tau} \right] = 0. \quad (46)$$

In the non-relativistic or weak gravity limit, the particle's velocity is sufficiently slow, i.e.  $v \ll c$  and in such a slow velocity situation the proper time  $\tau$  may be approximated to the coordinate time  $t$ . Hence, the spatial components of four velocity  $v^i = dx^i/dt \equiv (dx^1/dt, dx^2/dt, dx^3/dt) \ll dx^0/dt$  [31, 73, 74]. Thereby, it is seen from the above equation that the first term within the square bracket is negligible in comparison with the second term. So, in the weak field limit and for static spacetime the equation of motion contains radial component only. With the radial component of the geodesic equation, we get from equation (46) as given by

$$\frac{d^2 r}{dt^2} = - \left[ \tilde{\Gamma}_{00}^1 - \frac{\kappa}{\sqrt{6}} \frac{d\phi}{dr} \right]. \quad (47)$$

This is the equation of motion of the particle in the Einstein frame in the weak field approximation. It shows that the geodesic in this frame contains a term  $\kappa/\sqrt{6} (d\phi/dr)$  due to the scalaron field in addition to the gravitational term. This term can be defined as the acceleration caused by chameleon force  $F_{\phi}$  that appears as a result of the chameleonic nature of the scalaron field. Obviously, in the weak field limit, chameleon force exists and a test particle experiences chameleonic force apart from the gravitation force also. So, the dynamics of the test particle will be controlled by both of these two forces. Now, for simplicity, if we assume that the orbit of the particle is circular, the centripetal acceleration of the particle moving with velocity  $v$  will be

$$a = -\frac{v^2}{r}. \quad (48)$$

These two equations (47) and (48) result in the following velocity equation:

$$v^2 = r \left[ \tilde{\Gamma}_{00}^1 - \frac{\kappa}{\sqrt{6}} \frac{d\phi}{dr} \right]. \quad (49)$$

As in the weak field limit, the velocity of a particle is vanishingly small [75, 76] as discussed before, one may obtain

$$\Gamma_{00}^1 \simeq -\frac{1}{2} \frac{\partial g_{00}}{\partial r}. \quad (50)$$

Hence,

$$\tilde{\Gamma}_{00}^1 \simeq -\frac{1}{2} \frac{\partial \tilde{g}_{00}}{\partial r} \simeq -\frac{1}{2} \frac{\partial(\Omega^2 g_{00})}{\partial r}. \quad (51)$$

Next, to compute  $d\phi/dr$  we will use equation (28) and the metric (41). It can be expressed as

$$\frac{d\phi}{dr} = \frac{d\phi}{dR} \frac{dR}{dr}. \quad (52)$$



From the metric (41) Ricci scalar is obtained as

$$R = \frac{e^{-\nu}}{2r^2} \left[ -4 + 4e^\nu - r^2\mu'^2 + 4r\nu' + r\mu'(-4 + r\nu') - 2r^2\mu'' \right], \quad (53)$$

where the prime denotes the derivative with respect to the radial coordinate  $r$ . Thus

$$\frac{dR}{dr} = \frac{e^{-\nu}}{2r^3} \left[ 8 - 8e^\nu + r^3\mu'^2\nu + r\mu' \{ 4 + r(4\nu' - r\nu^2 + r(-2\mu'' + \nu'')) \} + r^2(-4\nu'^2 - 4\mu'' + 3r\nu'\mu'' + 4\nu'' - 2r\mu''') \right]. \quad (54)$$

It is clear from equations (51) and (54) that to have a precise velocity equation from equation (49), we need to derive the explicit forms of the  $e^\mu$  and  $e^\nu$  first. These coefficients will shape the velocity profile of the particle by determining  $dR/dr$  and  $\Gamma_{00}^1$  respectively.

In the said context, it is worth mentioning that the generalized field equation of an MTG can be recast in the form given below [20, 74, 77, 78]:

$$\xi(\varphi) [G_{\mu\nu} + X_{\mu\nu}] = \kappa^2 T_{\mu\nu}, \quad (55)$$

where  $X_{\mu\nu}$  is an additional term that appeared due to modification of geometry in an MTG,  $\xi(\varphi)$  is a coupling factor that couples geometry to matter,  $\varphi$  may be a curvature invariant or other gravitational field such as a scalar field. For  $X_{\mu\nu} = 0$  and  $\xi(\varphi) = 1$ , one can recover GR. In our case, we have equation (7) similar to generalized equation (55), where the coupling factor  $\xi(\varphi) = f_R$  and the tensor  $G_{\mu\nu}^d$  represents the modified term regarding GR. From the metric (41) and the generalized field equation (55), derivation of the metric coefficient  $e^\nu$  is accomplished in Refs. [20] and is found as

$$e^\nu = \left( 1 - \frac{2G\bar{M}(r)}{r} \right)^{-1} = \left( 1 - \frac{2GM(r)}{\Omega^2 r} \right)^{-1}, \quad (56)$$

where  $\bar{M}(r)$  denotes modified mass profile [20, 74] which is

$$\bar{M}(r) = \frac{M(r)}{\Omega^2} = \frac{1}{\Omega^2} \int_0^r \left( \frac{\kappa^2 \rho(r) r^2}{2Gf_R(r)} - \Omega^2 \frac{r^2 X_{00}(r)}{2Ge^\mu} \right) dr. \quad (57)$$

Equation (56) indicates the resemblance of the form of metric coefficient  $e^\nu$  to the standard Schwarzschild form. As in the limit  $r \rightarrow \infty$ , i.e. at very large distance from the source of the gravitation field (in our case from the center of the galaxy), the metric coefficients can plausibly be assumed in the standard Schwarzschild form. Therefore, we consider the weak field limit where the spacetime can be adopted as Minkowskian and thereby can be expressed  $\tilde{g}_{\mu\nu}$  in terms of Minkowski metric  $\eta_{\mu\nu}$  as [20, 71]

$$\tilde{g}_{\mu\nu} = \Omega^2 (\eta_{\mu\nu} + g_{\mu\nu}), \quad (58)$$

and we obtain  $g_{00} = -2\phi$  to the first order in  $g_{\mu\nu}$ , where  $\phi = G\bar{M}(r)/r = GM(r)/\Omega^2 r$ . Hence, we may write  $e^\mu$  from equation (58) as

$$e^\mu \approx 1 - \frac{2G\bar{M}(r)}{r} = 1 - \frac{2GM(r)}{\Omega^2 r}. \quad (59)$$

Thus,  $\tilde{\Gamma}_{00}^1$  of equation (51) takes the form:

$$\tilde{\Gamma}_{00}^1 = \frac{GM(r)}{r^2}. \quad (60)$$

On the other hand, we require derivatives of metric functions to get  $dR/dr$  exactly. On that account, the metric functions are written from (56) and (59) as

$$\nu(r) = \ln \left( 1 - \frac{2GM(r)}{\Omega^2 r} \right)^{-1}, \quad (61)$$

$$\mu(r) = \ln \left( 1 - \frac{2GM(r)}{\Omega^2 r} \right). \quad (62)$$

After performing derivations of these two equations with respect to  $r$  we are able to find

$$\nu' = - \left( \frac{2M(r)}{\Omega^2 r^2} - \frac{4M^2(r)}{\Omega^4 r^3} \right) e^{2\nu}, \quad \nu'' = \frac{4M(r)}{\Omega^2 r^3} e^\nu + \frac{4M^2(r)}{\Omega^4 r^4} e^{2\nu}. \quad (63)$$

$$\mu' = \frac{2M(r)}{\Omega^2 r^2} e^\nu, \quad \mu'' = - \frac{4M(r)}{\Omega^2 r^3} e^\nu - \frac{4M^2(r)}{\Omega^4 r^4} e^{2\nu}, \quad (64)$$

$$\mu''' = \frac{24M^2(r)}{\Omega^4 r^5} e^{2\nu} + \frac{12M(r)e^\nu}{\Omega^2 r^4} + \frac{16M^3(r)}{\Omega^6 r^6} e^{3\nu}. \quad (65)$$

On substitution of equations (56), (61) and (63) – (65) into equation (54) we attain the expression of  $d\phi/dr$  from equation (52) with the help of equation (28) after being carried out some algebraic calculations as given by

$$\frac{d\phi}{dr} = \frac{2\sqrt{6}f_{RR}}{r^3\kappa f_R} \left[ -1 + e^{-\nu} - \frac{2M^3(r)}{\Omega^6 r^3} e^{2\nu} - \frac{3M^2(r)}{\Omega^4 r^2} e^\nu + \frac{3M^2(r)}{\Omega^4 r^3} e^\nu + \frac{2M^3(r)}{\Omega^6 r^4} e^\nu + \frac{4M(r)}{\Omega^2 r} \right]. \quad (66)$$

Our purpose is to find the rotational velocity of a particle (star) according to equation (49). This is the equation of motion of a particle that follows the geodesic of metric  $g_{\mu\nu}$  basically under the static and weak field approximation of the gravitation field sourced by a galaxy. Thus, we obtain the rotational velocity equation for the particle by inserting equations (60) and (66) into equation (49), and also writing  $\Omega^2 = f_R$  as follows:

$$v^2 = \frac{GM(r)}{r} + \frac{2f_{RR}}{r^2 f_R} \left[ 1 - e^{-\nu} + \frac{2M^3(r)}{f_R^3 r^3} e^{2\nu} + \frac{3M^2(r)}{f_R^2 r^2} e^\nu - \frac{3M^2(r)}{f_R^2 r^3} e^\nu - \frac{2M^3(r)}{f_R^3 r^4} e^\nu - \frac{4M(r)}{r f_R} \right]. \quad (67)$$

We may write this equation as

$$v = \sqrt{v_{Neff}^2 + v_\phi^2},$$

where  $v_{Neff} = \sqrt{\frac{GM(r)}{r}}$  can be considered as the effective Newtonian velocity term and  $v_\phi$  as the velocity due to the contribution of chameleon field. The  $v_{Neff}$  is differ from the standard Newtonian velocity because the mass function  $M(r)$ , defined by the equation (57), is linked to the modification of gravity. Notably, we focus on a model of a spherically symmetric system (galaxy) with energy density  $\rho(r)$ . However, the case of spherical symmetry assumed here is only for the sake of simplicity, as all galaxies considered in this study may not have this geometry. Moreover, from the derivative of the mass distribution described by (57) with respect to  $r$ , we may obtain an expression for the energy density function  $\rho(r)$ . Since the choice of  $\rho(r)$  influences how mass is distributed within a system, therefore, by selecting an appropriate function for  $\rho(r)$  in equation (57), the mass distribution can be made equivalent to a simpler one. In this context, we can assume the following simple mass distribution in a galaxy instead of the complex distribution illustrated by the equation equation (57) [74]:

$$M(r) = M_0 \left[ \sqrt{\frac{r_0}{r_c}} \left( \frac{r}{r+r_c} \right) \right]^{3b}, \quad (68)$$

where  $r_0$  is the scale length,  $M_0$  and  $r_c$  are the total mass and core radius of the galaxy respectively.  $b$  is a parameter that determines the slope of the mass profiles of galaxies. The values of  $M_0$  and  $r_c$  will be estimated from the fitting of theoretical rotation curves with observational data of respective galaxies. It should be mentioned that the expression

$$\rho(r) = \frac{3M(r)}{4\pi r^3} \left[ b \left( \frac{r_c}{r+r_c} \right) + \frac{r^2 X_{00}(r)}{3(1-e^\mu)e^\mu} \right] f_R(r), \quad (69)$$

which can be obtained by equating  $\Omega^2 \bar{M}'(r) = \frac{\kappa^2 \rho(r) r^2}{2Gf_R(r)} - \Omega^2 \frac{r^2 X_{00}(r)}{2Ge^\mu}$  to  $M'(r) = \frac{3bM(r)r_c}{r(r+r_c)}$  is suitable one to make mass distributions (57) and (68) identical.

## B. Fitting of rotation curves and estimation of parameters

The rotational velocity of a particle rotating around the galactic center have been derived in the last subsection based on a recently introduced new  $f(R)$  gravity model (33). We generate rotation curves for the test particle according to equation (67) and intend to examine the influence of scalaron on rotational profiles to explain galactic

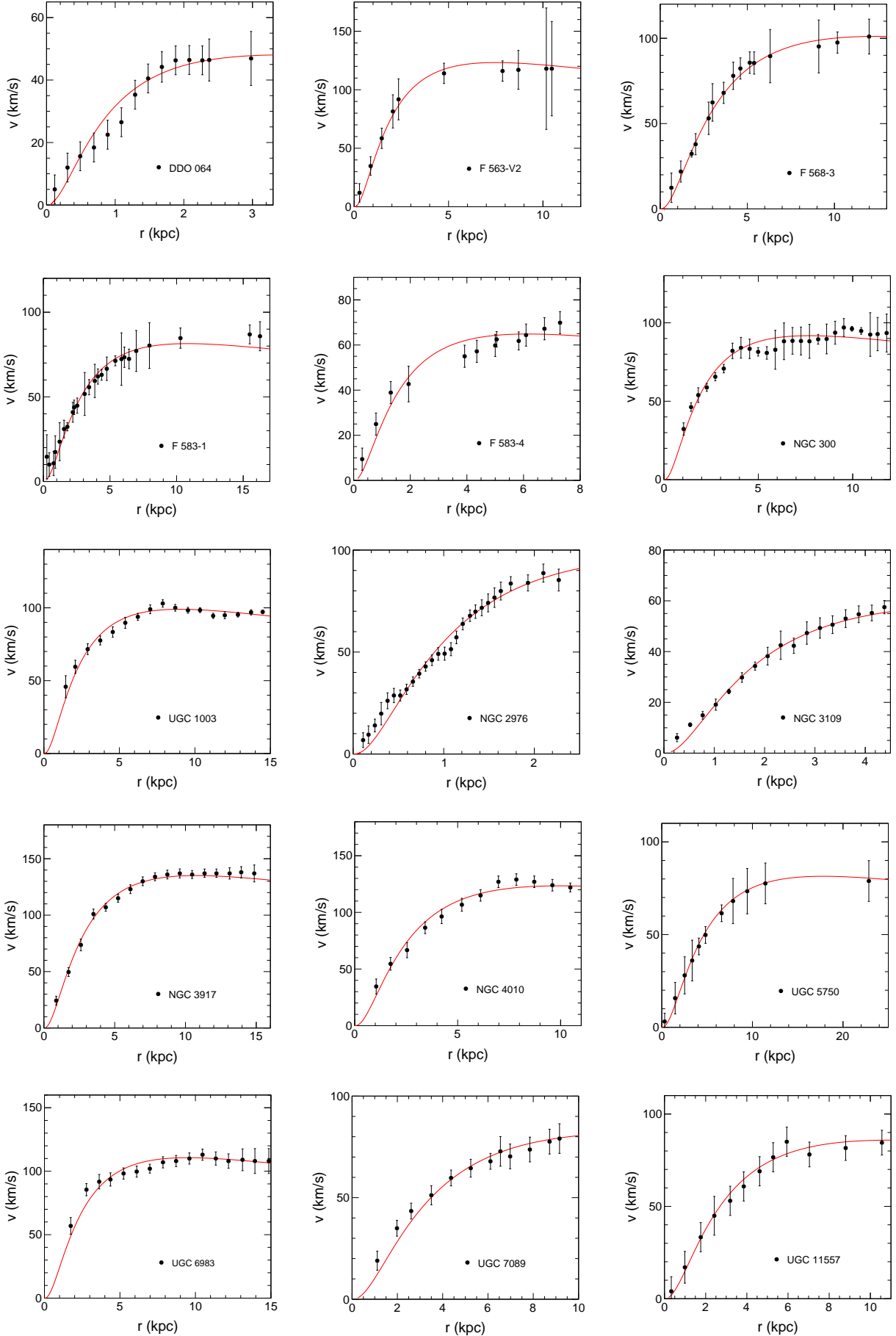


FIG. 2: Fitting of rotation curves generated from the  $f(R)$  gravity model (33) for rotation velocities of a sample of 15 LSB

TABLE I: Different physical properties of a set of fifteen observed LSB galaxies and the best-fitted values of total mass  $M_0$  and core radius  $r_c$  of each galaxy for the  $f(R)$  gravity model (33).

| Galaxy Name | Scale length<br>$r_0$ (kpc) | Distance $D$<br>(Mpc) | Luminosity $L_B$<br>( $10^{10} L_\odot$ ) | Mass $M_0$<br>( $10^{10} M_\odot$ ) | Core Radius<br>$r_c$ (kpc) | $\chi_{red}^2$ |
|-------------|-----------------------------|-----------------------|---|-------------------------------------|----------------------------|----------------|
| DDO 064     | 0.69                        | 6.8                   | 0.015                                     | 4.1                                 | 2.04                       | 0.53           |
| F563-V2     | 2.43                        | 59.7                  | 0.266                                     | 2.00                                | 1.50                       | 2.20           |
| F 568-3     | 4.99                        | 82.4                  | 0.351                                     | 1.20                                | 2.50                       | 0.42           |
| F 583-1     | 2.36                        | 35.4                  | 0.064                                     | 4.10                                | 2.16                       | 0.39           |
| F 583-4     | 1.93                        | 53.3                  | 0.096                                     | 0.50                                | 1.23                       | 0.33           |
| NGC 300     | 1.75                        | 2.08                  | 0.271                                     | 3.30                                | 1.54                       | 1.50           |
| NGC 2976    | 1.01                        | 3.58                  | 0.201                                     | 1.01                                | 0.84                       | 0.92           |
| NGC 3109    | 1.56                        | 1.33                  | 0.064                                     | 1.50                                | 1.45                       | 1.50           |
| NGC 3917    | 2.63                        | 18.0                  | 1.334                                     | 8.00                                | 2.15                       | 5.10           |
| NGC 4010    | 2.81                        | 18.0                  | 0.883                                     | 4.10                                | 2.00                       | 0.20           |
| NGC 1003    | 1.61                        | 11.4                  | 1.480                                     | 5.60                                | 1.80                       | 0.09           |
| UGC 5750    | 3.46                        | 58.7                  | 0.472                                     | 9.60                                | 3.56                       | 0.31           |
| UGC 6983    | 3.21                        | 18.0                  | 0.577                                     | 1.80                                | 1.90                       | 1.50           |
| UGC 7089    | 2.26                        | 18.0                  | 0.352                                     | 11.6                                | 2.70                       | 0.24           |
| UGC 11557   | 2.75                        | 24.2                  | 1.806                                     | 3.10                                | 2.20                       | 0.59           |

TABLE II: Different physical properties of a set of ten observed HSB galaxies and the best-fitted values of total mass  $M_0$  and core radius  $r_c$  of each galaxy for the  $f(R)$  gravity model (33).

| Galaxy Name | Scale length<br>$r_0$ (kpc) | Distance $D$<br>(Mpc) | Luminosity $L_B$<br>( $10^{10} L_\odot$ ) | Mass $M_0$<br>( $10^{10} M_\odot$ ) | Core Radius<br>$r_c$ (kpc) | $\chi_{red}^2$ |
|-------------|-----------------------------|-----------------------|---|-------------------------------------|----------------------------|----------------|
| NGC 2903    | 2.33                        | 6.6                   | 4.088                                     | 23.00                               | 2.50                       | 4.50           |
| NGC 2998    | 6.20                        | 68.1                  | 5.186                                     | 16.00                               | 3.90                       | 1.04           |
| NGC 3198    | 3.14                        | 13.8                  | 3.241                                     | 102.50                              | 6.70                       | 1.20           |
| NGC 3769    | 3.38                        | 18.0                  | 0.684                                     | 22.80                               | 4.90                       | 0.12           |
| NGC 4088    | 2.58                        | 18.0                  | 2.957                                     | 69.40                               | 5.00                       | 0.62           |
| NGC 4157    | 2.32                        | 18.0                  | 2.901                                     | 81.60                               | 4.46                       | 1.91           |
| NGC 4183    | 2.79                        | 18.0                  | 1.042                                     | 29.00                               | 5.25                       | 1.70           |
| NGC 4217    | 2.94                        | 18.0                  | 3.031                                     | 57.20                               | 4.70                       | 0.71           |
| NGC 5055    | 3.20                        | 9.9                   | 3.622                                     | 56.00                               | 4.50                       | 0.41           |
| NGC 7793    | 1.21                        | 3.61                  | 0.910                                     | 20.00                               | 2.80                       | 3.06           |

dynamics in the absence of dark matter by fitting the theoretically predicted curves with the observational data of a sample of 37 galaxies including fifteen LSB, ten HSB and twelve dwarf galaxies [79].

It is noteworthy that LSB galaxies are slowly evolving objects that have DM domination in all radii. They live in less dense, extremely extended DM halos and are found to be more isolated relative to HSB galaxies [80, 81]. Refs. [82–84] have analyzed that the rotation curves of LSB and Dwarf galaxies are slowly rising, shallower at small radii. Contrary to this, an HSB galaxy has a higher central mass density that leads to a steeply rising rotation curve in the inner region followed by a relatively flat outer part [85]. Taking note of these results, rotation curves for all these

TABLE III: Different physical properties of a set of twelve observed dwarf galaxies and the best-fitted values of total mass  $M_0$  and core radius  $r_c$  of each galaxy for the  $f(R)$  gravity model (33).

| Galaxy Name | Scale length<br>$r_0$ (kpc) | Distance ( $D$ )<br>(Mpc) | Luminosity ( $L_B$ )<br>$10^{10}L_\odot$ | Mass ( $M_0$ )<br>$10^{10}M_\odot$ | Core Radius<br>$r_c$ (kpc) | $\chi^2_{red}$ |
|-------------|-----------------------------|---------------------------|--|------------------------------------|----------------------------|----------------|
| NGC 2366    | 0.65                        | 3.27                      | 0.236                                    | 5.44                               | 1.10                       | 5.04           |
| NGC 3877    | 2.53                        | 18.0                      | 1.948                                    | 6.00                               | 1.72                       | 4.60           |
| NGC 3972    | 2.18                        | 18.0                      | 0.978                                    | 7.40                               | 1.85                       | 1.20           |
| NGC 5585    | 1.53                        | 7.06                      | 0.333                                    | 5.40                               | 1.60                       | 4.90           |
| UGC 4325    | 1.86                        | 9.6                       | 2.026                                    | 0.25                               | 0.84                       | 7.10           |
| UGC 4499    | 1.73                        | 12.5                      | 1.552                                    | 1.40                               | 1.38                       | 2.01           |
| UGC 6446    | 1.49                        | 12.0                      | 0.988                                    | 2.00                               | 1.28                       | 0.54           |
| UGC 6667    | 5.15                        | 18.0                      | 0.422                                    | 0.13                               | 1.60                       | 2.20           |
| UGC 6818    | 1.39                        | 18.0                      | 0.352                                    | 9.00                               | 1.90                       | 0.96           |
| UGC 6917    | 2.76                        | 18.0                      | 6.832                                    | 0.92                               | 1.50                       | 1.20           |
| UGC 7524    | 3.46                        | 4.74                      | 2.436                                    | 0.90                               | 2.00                       | 0.77           |
| UGC 12632   | 2.42                        | 9.77                      | 1.301                                    | 1.06                               | 1.68                       | 0.70           |

three types of galaxies are produced and fitted by considering a predetermined set of model parameters  $\alpha = 0.0005$  and  $R/R_c = 2$  from Ref. [28] for all the samples. Also, another model parameter  $\beta$  is set to 0.0001 for each galaxy, and fitting of theoretical curves is carried out by constraining parameters  $M_0$  and  $r_c$  using the best-fitted values for each sample galaxy. As already mentioned the parameter  $b$  determines the slope of the mass profile (68). Higher values of  $b$  produce a more slowly rising mass profile, whereas lower values yield a steeply rising mass profile leading respectively gradually and steeply rising rotation curves of galaxies. These two characteristics are indicative of LSB and Dwarf galaxies, and HSB galaxies, respectively. We have analyzed the value of  $b$  by allowing it to be a free parameter in the fitting of the predicted rotation curves defined by equation (67) and observed that  $b = 1$  provides a good fit for the steeply rising rotation curves of HSB galaxies, whereas  $b = 2$  tends to fit slowly rising shallower at small radii curves of the LSB and Dwarf galaxies. Hence, similar to Refs. [58, 74] the value of the parameter  $b$  is taken as 1 for HSB and it is 2 for both LSB and Dwarf galaxies. After fitting a notable agreement between predictions and actual observations is observed for all samples. These perfectly matched rotation curves with observational data, extracted from Ref. [79], estimate the values of  $M_0$  and  $r_c$  well and are obtained as per the characteristics of different classes of galaxies. The LSB galaxies can be fitted from a maximum radial distance 2.5 kpc to 22.5 kpc. Similarly, HSB galaxies' maximum fitted radial distance varies from 6 kpc to 30 kpc and in the case of dwarf galaxies it is from 6 kpc to 12 kpc. In Tables I, II and III, the successfully fitted values of  $M_0$  and  $r_c$  are listed together with some other galactic parameters extracted from Ref. [54] and reduced  $\chi^2$  values of fitting for different galaxies. From the tables, it is seen that for HSB galaxies total mass  $M_0$ , in the solar mass unit (here we consider  $M_0 = 10^{10}M_\odot$ ), is large and in the case of LSB and dwarf galaxies this value is small.

The behavior of galactic rotation curves of 37 sample galaxies are presented in Figs. 2, 3 and 4 respectively. Furthermore, we are endeavoring to understand the effectiveness of the chameleon field on the dynamics of galaxies. For this purpose, we plot the difference between the velocity determined by equation (67) and the effective Newtonian velocity  $\sqrt{GM(r)/r}$  as a function of radial distance  $r$  for 6 sample galaxies taking two from each category LSB, HSB and Dwarf (see Fig. 5) utilizing the values of model parameters that have already been taken into account and the same values of  $M_0$  and  $r_c$  obtained from Tables I, II and III of respective galaxies. It is observed from Fig. 5 that the difference between these two velocities is not noticeably large. This result suggests a marginal impact of the chameleon field on galactic rotation curves. Contrarily, the major contribution to rotation curves is found due to the effective Newtonian velocity term which depends not only on the distance  $r$  but also on the mass function  $M(r)$  specified identically by the equation (68) and is connected to density profile (69). Therefore, this velocity  $v_{Neff}$  contributes significantly to account for the observed rotation curves, without the need for dark matter. As the chameleon mechanism acts as a screening mechanism, so in regions of high matter density, like galaxies, the chameleon field becomes effectively screened off, thereby its influence may reduce in the galactic environment. This screening mechanism ensures a minimal impact of the chameleon field on galactic dynamics. Thus, the behavior of rotation curves

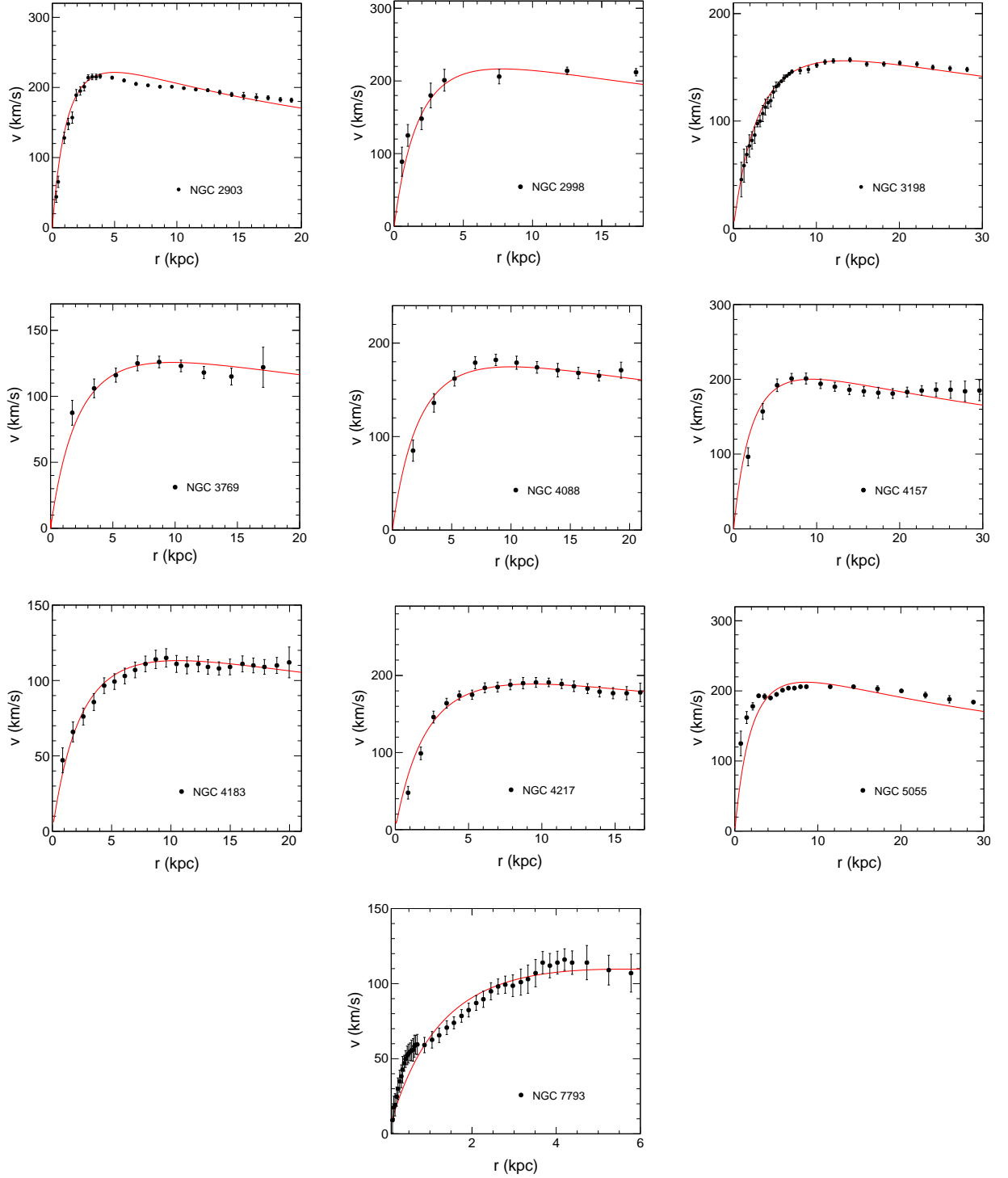


FIG. 3: Fitting of rotation curves generated from the  $f(R)$  gravity model (33) for rotation velocities of a sample of 10 HSB galaxies with their quoted errors. The data points are observational values of rotational velocities extracted from Ref. [79].

through modification of gravity with a scalar field attributing chameleonic nature can be illustrated using the newly introduced  $f(R)$  model.

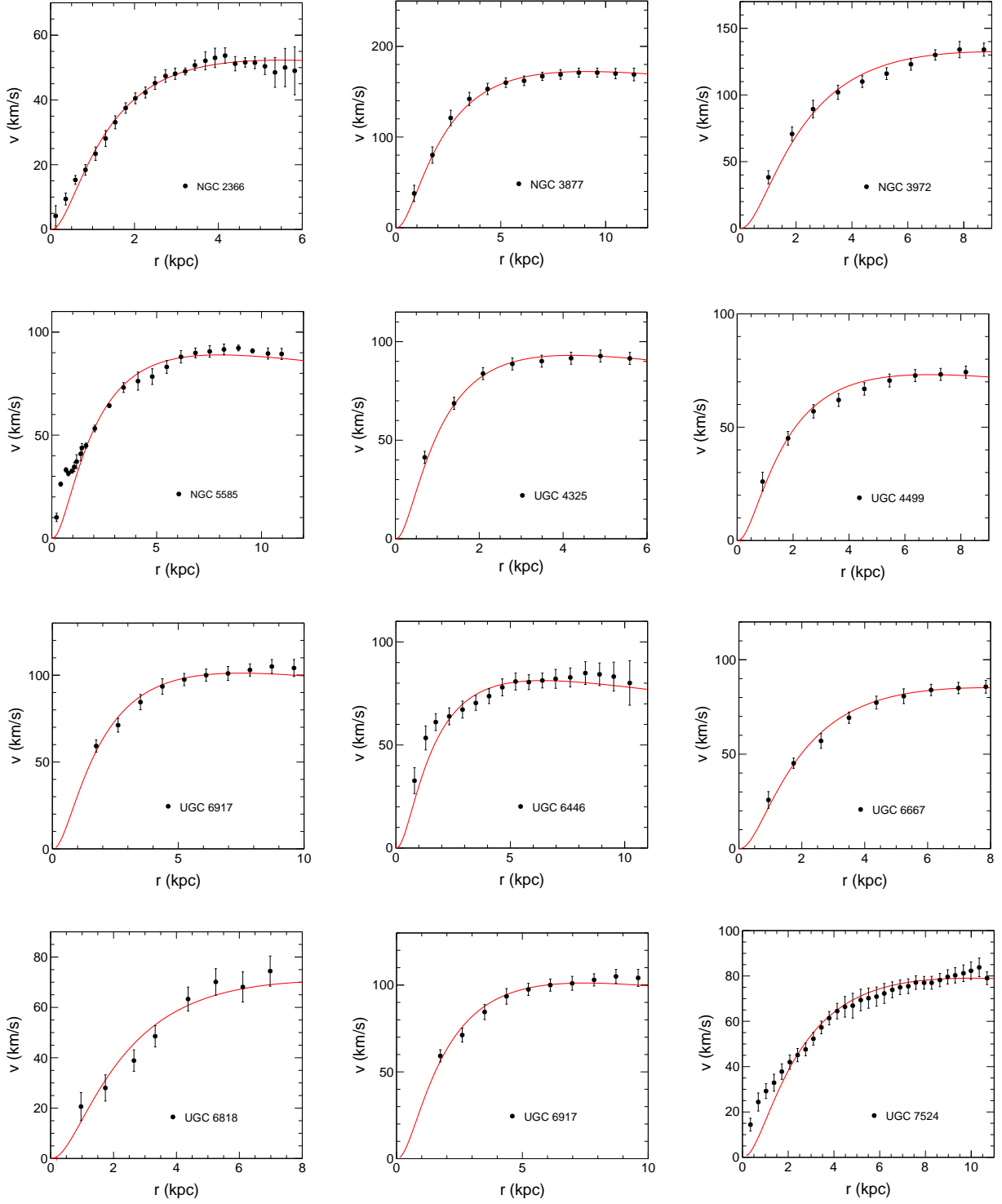


FIG. 4: Fitting of rotation curves generated from the  $f(R)$  gravity model (33) for rotation velocities of a sample of 12 dwarf galaxies with their quoted errors. The data points are observational values of rotational velocities extracted from Ref. [79].

## V. CONCLUSIONS

The DM issue is one of the greatest theoretical difficulties in modern physics in general and astrophysics in particular. Usually, the unique behavior of galactic rotation curves is interpreted by postulating the existence of this invisible matter distributed in a spherical halo around the galaxies. Of course, lack of acceptable evidences of such

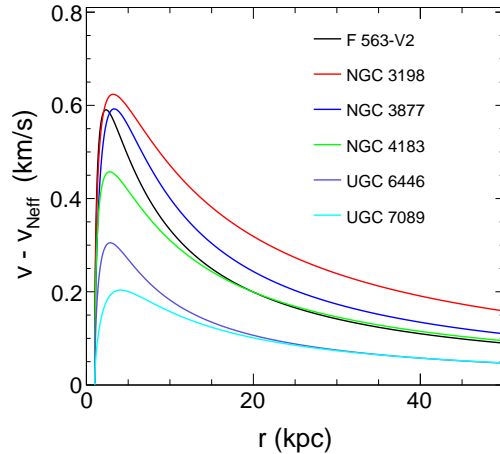


FIG. 5: Difference of velocity  $V$  and effective Newtonian velocity  $V_{Neff}$  i.e.,  $(V - V_{Neff})$  against radial distance  $r$ .  $V$  is derived from equation (67) and  $V_{Neff} = \sqrt{GM(r)/r}$ .

matter, modification of gravity is considered as a reasonable alternative for the explanation of observed galactic rotation curves. Looking into this, we thought about a popular and one of the simplest MTGs, the  $f(R)$  gravity, for our study. Within the framework of this gravity, Refs. [20, 56, 86] have implemented the theory to study galactic dynamics. Ref. [20] employs the Palatini formalism along with the Weyl transformation and discusses rotation curves of different galaxies including an ultra diffuse galaxy. Ref. [56] has studied the effect of chameleon  $f(R)$  gravity on rotation curves and radial acceleration relations of disc galaxies. In our work utilizing the metric formalism of the theory we have investigated the impact of the scalaron on rotation curves and addressed singularity issue (in Appendix A) faced by the  $f(R)$  model considered. For this the field equations are derived first and then obtained the equation for the extra degree of freedom  $f_R$  taking the trace of the field equation. To identify  $f_R$  as a scalar field (scalaron), we used conformal transformation, then tried to check the viability of a recently introduced  $f(R)$  model, regarding the chameleonic behavior. For this relation between chameleon mass  $m_\phi$  and local matter density  $\rho$  is established in equation (39). Fig. 1 illustrates this relationship and shows the growth of  $m_\phi$  with  $\kappa\rho$ , indicating higher  $m_\phi$  in regions of high density and lower in low density regions. The variation of chameleon mass is a consequence of the interaction of chameleon field with matter.

Then we aimed to investigate the effect of scalaron on the rotation curves of galaxies. For this, by considering a star as a test particle in a static spherically symmetric spacetime we have derived the rotation velocity equation (67) of the particle moving around the galactic center in Einstein frame. This equation demonstrates the influence of both effective Newtonian gravity and the chameleon force  $F_\phi$  on the motion of the particle. The effective Newtonian gravity term in equation (67) arises according to equations (49) and (60). Contribution of  $F_\phi$  in the second term emerges from the variation of the chameleon field  $\phi$  with radial distance  $r$ , as described by equation (49) and (66). To illustrate the galactic dynamics resulting from the combined effects of these forces, we have generated rotation curves for 37 galaxies using equation (67) to determine the rotational velocity of particles in stable circular orbits. To test the model we fit equation (67) with observational rotation curve data extracted from Ref. [79]. In all cases we observe a remarkable match between the model and the observations. Total mass  $M_0$  and the core radius  $r_c$  are determined for each galaxy from the fitting of predicted rotation curves to observed data of the sample galaxies by employing the  $\chi^2$  minimization technique. The  $\chi^2_{red}$  values are displayed in respective tables against each galaxy. It is seen that the  $\chi^2_{red}$  values are not equivalent or close to 1 relative to all the galaxies. In case of galaxies NGC 2366, NGC 2903, NGC 7793, UGC 4325, NGC 3877 and NGC 5585, its value is quite larger than 1. Still, we can almost fit the curves successfully where the predicted curves exhibit a nice and good agreement with the observed curves as shown in respective figures. Moreover, in order to comprehend the extent of the impact of scalaron, we have depicted velocity difference curves of 6 galaxies two each from the LSB, HSB and dwarf with respect to radial distance  $r$  for similar values of model parameters  $\alpha, \beta$  and of  $M_0$  and  $r_c$  estimated by the best-fitted curves of respective galaxies. Significantly, this plot does not suggest a notable influence of the scalaron on galactic dynamics. It is due to the screening characteristic of the chameleon mechanism for which in high matter density regions such as around massive objects like galaxies, the chameleon field becomes effectively screened resulting in a small acceleration of the field. For this, its influence is reduced on the motion of a particle around the center of a galaxy.

Hence, we may conclude that alternative of an explicit form of dark matter can be addressed by means of chameleon  $f(R)$  gravity theory. However, in contrast to the approach centered on the single mass model, there



are possibilities for comparative study by considering different mass profiles derived from the density distributions such as Navarro-Frenk-White (NFW), pseudo-isothermal (ISO) [87–89] etc. with other convenient modified gravity models. We aim to develop the work further sustaining this viewpoint in the future.

### Acknowledgements

UDG is thankful to the Inter-University Centre for Astronomy and Astrophysics (IUCAA), Pune, India for the Visiting Associateship of the institute.

### Appendix A: Singularity problem and its correction

To understand the singularity problem in the specific new  $f(R)$  gravity model chosen for our study, initially, we take the field-dependent scalaron potential without matter contribution which is attained in the form:

$$\frac{V(\phi)}{V_0} = \left[ \frac{\alpha}{2} + \beta - \left( \frac{2\alpha}{\pi} \right)^{1/3} \left( 1 - e^{\sqrt{\frac{2}{3}}\kappa\phi} \right)^{2/3} \right] e^{-2\sqrt{\frac{2}{3}}\kappa\phi}, \quad (\text{A1})$$

where  $V_0 = R_c/2\kappa^2$  is the normalization factor that normalizes the potential  $V(\phi)$ . The relation between  $V(\phi)$  and  $\phi$  given in equation (A1) is shown in Fig. 6.

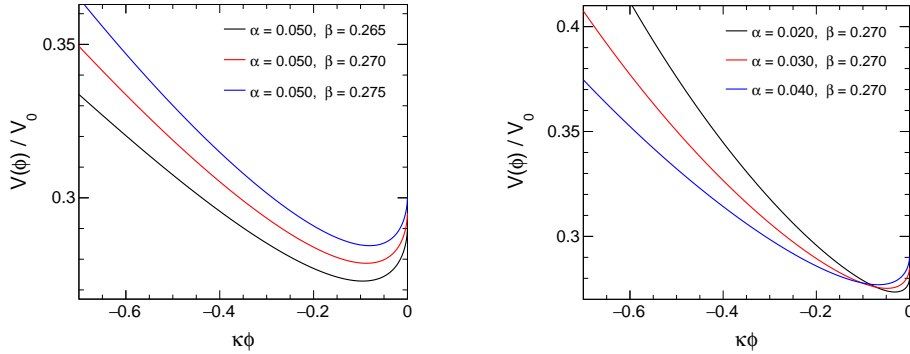


FIG. 6: Variation of  $V(\phi)$  with respect to  $\kappa\phi$  for different values of model parameters  $\alpha$  and  $\beta$  with  $R_c = 1$

In the left panel, we depict an explicit behavior of the potential as a function of the field and see that the potential decreases with increasing  $\phi$ . It reaches a minimum at  $\phi \sim -0.1$  and then increases up to  $\phi = 0$ . This behavior of the potential reflects the dynamics of the field  $\phi$  indicating that the scalaron is rolling down in the slope of the potential, and potential minimum at  $\phi \sim -0.1$  suggests a stable equilibrium position of the field. The other two panels illustrate that the minimum of the potential moves towards the higher field value for larger values of  $\alpha$  and  $\beta$ . Also, the potential minimum uplifts noticeably for higher values of  $\alpha$  and  $\beta$ .

Now, we consider the matter contribution to the potential as obtained from equation (25) and plot the behavior of the effective potential in Fig. 7 against the scalaron field for a positive matter density using the normalized equation as given below:

$$\frac{V_{eff}(\phi)}{V_0} = \left[ \frac{\alpha}{2} + \beta - \left( \frac{2\alpha}{\pi} \right)^{1/3} \left( 1 - e^{\sqrt{\frac{2}{3}}\kappa\phi} \right)^{2/3} + \frac{\rho\kappa^2}{2R_c} \right] e^{-2\sqrt{\frac{2}{3}}\kappa\phi}. \quad (\text{A2})$$

One can see from Fig. 7 that the presence of matter flattened the minimum of the potential and shifted it very close to  $\phi = 0$ . In fact, the minimum can smoothly correspond to zero of the scalaron field. This  $\phi \rightarrow 0$  correlates with the curvature singularity as hinted by equation (69) i.e.,  $R \rightarrow \infty$  when  $\phi \rightarrow 0$ , can be easily obtainable in the presence of matter. Ref. [70] suggested that the problem of curvature singularity is not unique to only a particular  $f(R)$  gravity model, but it is endured by many infrared-modified  $f(R)$  gravity models.

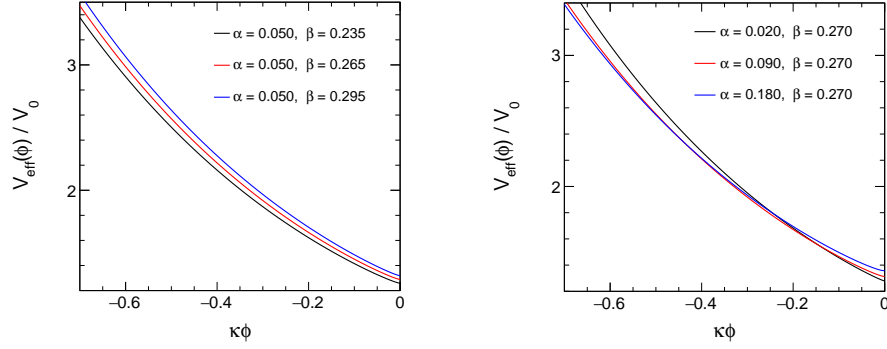


FIG. 7: Variation of effective potential  $V_{eff}(\phi)$  as a function of  $\kappa\phi$  for different values of model parameters  $\alpha$  and  $\beta$  with the matter density  $\rho = \rho_c$ , where  $\rho_c$  is the critical matter density of the Universe and  $R_c = 1$ .

The above curvature singularity appeared in terms of the scalaron field potential in the large curvature regime can be removed by reforming the structure of the potential in this curvature regime. This can be done by adding higher order correction term to the  $f(R)$  model as follows [19, 52, 90–93]:

$$f(R) = R - \frac{\alpha}{\pi} R_c \cot^{-1}\left(\frac{R_c^2}{R^2}\right) - \beta R_c \left[1 - e^{-\frac{R}{R_c}}\right] + \sigma R^2, \quad (\text{A3})$$

where  $\sigma$  is a dimensional constant. In the higher curvature regime equation (A3) may reduce to [19, 52]

$$f(R) \approx R - \frac{\alpha R_c}{2} - \beta R_c + \sigma R^2. \quad (\text{A4})$$

Also, after introducing the correction term we obtain  $f_R$  and the relation between curvature  $R$  and the scalaron field through conformal transformation respectively as follows:

$$f_R(R) = 1 - \frac{2\alpha R_c^3}{\pi R^3} - \beta e^{-\frac{R}{R_c}} + 2\sigma R, \quad (\text{A5})$$

$$e^{\sqrt{\frac{2}{3}}\kappa\phi} = 1 - \frac{2\alpha R_c^3}{\pi R^3} - \beta e^{-\frac{R}{R_c}} + 2\sigma R. \quad (\text{A6})$$

The noteworthy feature of this equation is that contrary to the resolution provided by the equation (69), it results in  $R \rightarrow \infty$  for  $\phi \rightarrow \infty$ . Equations (A4), (A5) and (A6) configure the  $R^2$  corrected normalized field potential as

$$\frac{V(\phi)}{V_0} = \left[ \frac{\alpha}{2} + \beta + \frac{7}{64\sigma R_c} (e^{\sqrt{\frac{2}{3}}\kappa\phi} - 1)^2 \right] e^{-2\sqrt{\frac{2}{3}}\kappa\phi}. \quad (\text{A7})$$

The potential given by this equation (A7) is plotted as a function of  $\kappa\phi$  with  $\sigma = 10^{-6} R_c^{-1} \text{ GeV}^{-2}$  and for different values of the parameters of the new  $f(R)$  gravity model in the left panel of Fig. 8. The figure shows that in the large curvature regime the potential is modified and attains a definite value. At  $\phi = 0$ ,  $R$  takes a small value  $\approx (\alpha R_c^3 / \pi \sigma)^{1/4}$  instead of infinity as expected.

Then, by considering the matter contribution, the equation for the  $R^2$  corrected effective potential is derived and obtained in the following normalized form:

$$\frac{V_{eff}(\phi)}{V_0} = \left[ \frac{\alpha}{2} + \beta + \frac{7}{64\sigma R_c} (e^{\sqrt{\frac{2}{3}}\kappa\phi} - 1)^2 + \frac{\rho\kappa^2}{2R_c} \right] e^{-2\sqrt{\frac{2}{3}}\kappa\phi}. \quad (\text{A8})$$

The variation of this effective potential (A8) is depicted in the right panel of Fig. 8 for four matter distributions. It exhibits that the effective potential achieves specific values in the high matter density regions (large curvature regions). Moreover, it is seen that the minimum of effective potential gradually becomes shallower as its position rises up and moves towards higher field values with the increasing matter densities, and finally it goes up to the plateau for the very high density environment. Thus, there is no possibility to have the curvature singularity after the  $R^2$  correction in our working model.

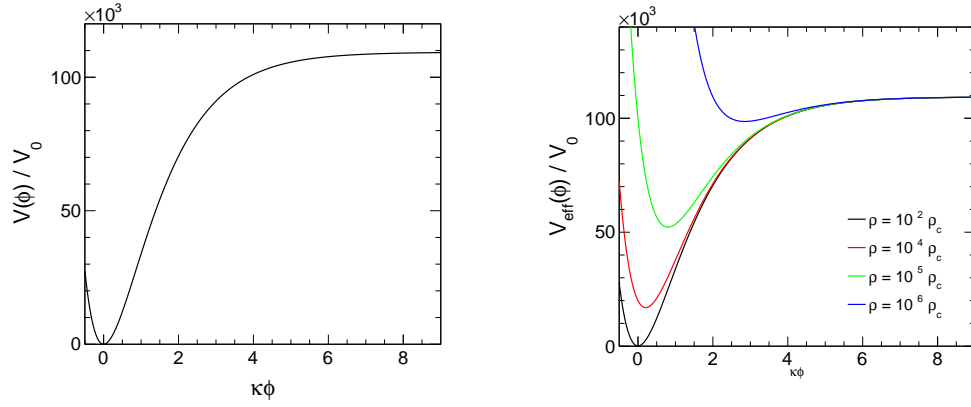


FIG. 8: Plot of  $R^2$  corrected potential  $V(\phi)$  as a function of  $\kappa\phi$  (left) and variation of  $R^2$  corrected effective potential  $V_{eff}(\phi)$  as a function of  $\kappa\phi$  for four positive values of matter density (right), where  $\rho_c$  is critical density of the Universe. Values of  $\alpha$ ,  $\beta$  and  $R_c$  are taken as 0.05, 0.25 and 1 respectively for both the cases.

Here, it is to be noted that we realized very high scalaron mass in high-density regions according to equation (39) (see Fig. 1) basically due to the singularity problem. Now, the singularity correction in the model modifies mass relation (39) into the following form provided  $R_0$  is as given by equation (38):

$$m_\phi^2 = \frac{\pi R_0^4}{3} \left[ R_c \left( 6\alpha R_c^4 + \pi R_0^4 (\beta e^{-R_0/R_c} + 2\sigma R_c) \right)^{-1} - \left( \pi R_0^3 (1 - \beta e^{-R_0/R_c} + 2\sigma R_0) - 2\alpha R_c^3 \right)^{-1} \right]. \quad (\text{A9})$$

In order to compare the mass represented by the equation (A9) to the previous one predicted by equation (39), we present Fig. 9 which illustrates the change in the mass of scalaron with the density of the environment for three different sets of model parameters  $\alpha$  and  $\beta$  as considered before the correction. The figure indicates a reasonably lighter scalaron for the same environment after the singularity correction of the model. Moreover, a notable decrease in mass is observed in both scenarios with varying  $\alpha$  and  $\beta$  values.

In a region where  $R_c < R < 1/\sigma$ , scalaron mass will be [52]

$$m_\phi^2 \approx \frac{1}{6\sigma}. \quad (\text{A10})$$

Equation (A10) indicates that the scalaron mass becomes stable within a range of considerable degree of curvature and is given by  $m_\phi \propto 1/\sigma$ , so it is completely controlled by the parameter  $\sigma$ . On the other hand, in an extremely high curvature regime i.e., at  $R \gg R_c$  (and  $R \gg \frac{1}{\sigma}$ ) scalaron's mass is obtained as [19, 52]

$$m_\phi^2 \approx \frac{1}{6\sigma(1 + 2\sigma R)}. \quad (\text{A11})$$

It hints at the possibility that the scalaron experiences a reduction in mass within regions of high curvature. It is worth mentioning that according to the analysis of Ref. [52] the upper boundary for the scalaron mass must be  $< \mathcal{O}(1)$  GeV. Our analysis yields a suitable result within this prescribed limit.

Thus, after resolving this problem the scalaron can be made fairly lighter instead of extremely heavier. The cause of this attribution is seen clearly from Fig. 10 that the potential pushes the scalaron field to obtain larger values in denser environments and also, as mentioned already, the minimum of effective potential becomes shallower in the high-density region after fixing the singularity problem suffered by the model.

Units of  $m_\phi$ : 1) Considering equation (39), we proceed with the dimensional analysis as given below. As previously mention, we have set  $\hbar = c = 1$ . i.e., we have chosen the natural unit system which ensures that all basic quantities namely mass, length, time, energy can be expressed in terms of single mass unit as

$$\text{mass} = \text{length}^{-1} = \text{time}^{-1} = \text{energy},$$

where unit of mass, length, time and energy are GeV,  $\text{GeV}^{-1}$ ,  $\text{GeV}^{-1}$  and GeV respectively. In our equation constants  $\alpha$ ,  $\beta$ ,  $\pi$  have no dimensions and  $e^{-\frac{R_0}{R_c}}$  is also a dimensionless term. Dimensions of other associated quantities are

$$[\rho] = [ML^{-3}], \quad [\kappa] = [M^{-1}L^3T^{-2}], \quad [\rho\kappa^2] = [T^{-2}], \quad [R_c] = [R_0] = [L^{-2}].$$

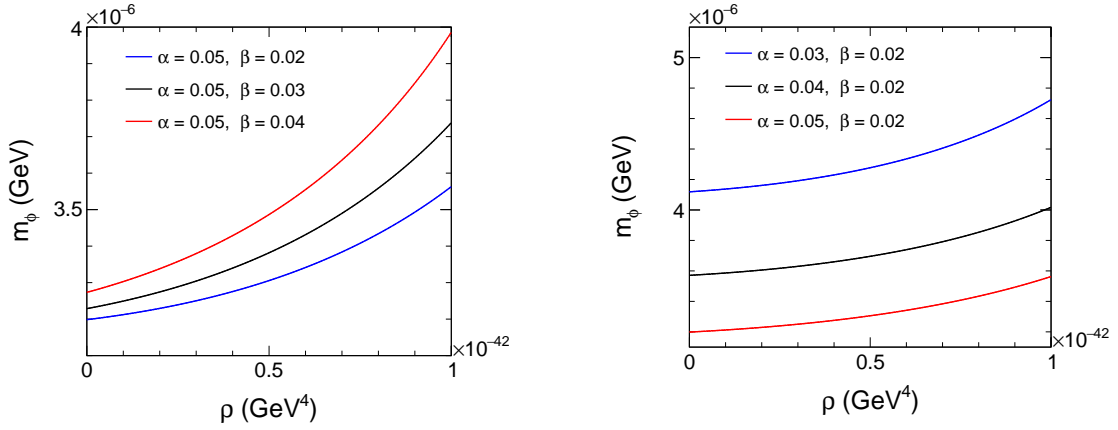


FIG. 9: Relations between scalaron mass and matter density for three sets of model parameters  $\alpha$  and  $\beta$  after singularity correction. The left plot is for different values of  $\beta$  by fixing  $\alpha$  to 0.05 and the right plot is for different values of  $\alpha$  by fixing  $\beta$  to a value 0.02. In both cases with  $R_c$  is set to 1.

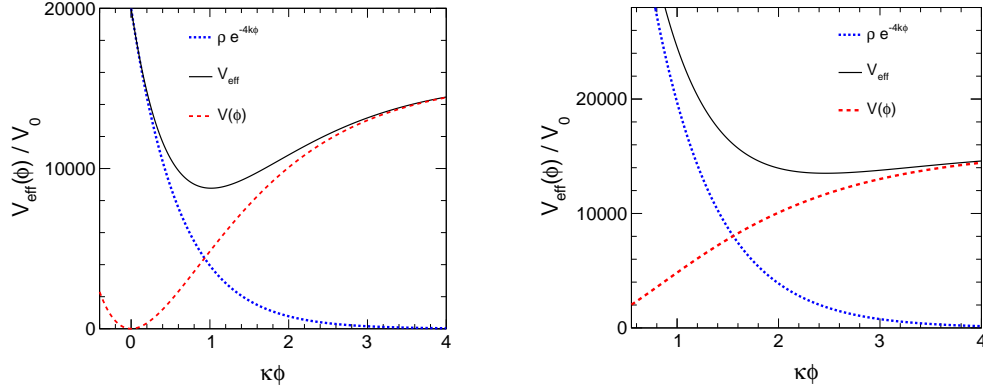


FIG. 10:  $R^2$  corrected scalaron effective potential  $V_{eff}(\phi)$  (black solid line) for the considered  $f(R)$  gravity model with respect to two matter distributions  $\rho \sim 10^4 \rho_c$  (left) and  $\rho \sim 10^5 \rho_c$  (right) respectively with  $R_c = 1$ . The red dashed lines show the contributions from the original potential and the blue dotted lines represent the contributions of the density-dependent term.

Therefore,

$$[(\rho\kappa^2 + \alpha R_c + 2\beta R_c)^4] = [L^{-8}], \quad \left[ \frac{R_c}{6\alpha R_c^4 + \pi\beta(\rho\kappa^2 + \alpha R_c + 2\beta R_c)^4 e^{-\frac{R_0}{R_c}}} \right] = [L^6],$$

$$\left[ \frac{1}{\pi(\rho\kappa^2 + \alpha R_c + 2\beta R_c)^3 [1 - \beta e^{-\frac{R_0}{R_c}}] - 2\alpha R_c^3} \right] = [L^6].$$

Hence,

$$\left[ \frac{R_c}{6\alpha R_c^4 + \pi\beta(\rho\kappa^2 + \alpha R_c + 2\beta R_c)^4 e^{-\frac{R_0}{R_c}}} - \frac{1}{\pi(\rho\kappa^2 + \alpha R_c + 2\beta R_c)^3 [1 - \beta e^{-\frac{R_0}{R_c}}] - 2\alpha R_c^3} \right] = [L^6].$$

These lead the dimension of right hand side =  $[L^{-8}][L^6] = [L^{-2}]$ . Thus,  $[m_\phi^2] = [L^{-2}]$ . This gives

$$[m_\phi] = [L^{-1}].$$

Hence,  $m_\phi$  can be expressed in  $(\text{GeV}^{-1})^{-1} = \text{GeV}$  unit.

2) Similarly in the case of equation (A9) dimensions of respective terms are same as  $[2\sigma R_c]$  has no dimension. Consequently, unit of mass is GeV in this case also.

**Appendix B: Derivation of equations (A7) – (A11):**

After  $R^2$  correction we obtain  $f_{RR}$  along with equations (A4) and (A5) as follows:

$$f_{RR}(R) = \frac{6\alpha R_c^3}{\pi R^4} + \frac{\beta}{R_c} e^{-\frac{R}{R_c}} + 2\sigma. \quad (\text{B1})$$

Now, using equation (16) and (A5) we may write

$$\begin{aligned} e^{\sqrt{\frac{2}{3}}\kappa\phi} &= 1 - \frac{2\alpha R_c^3}{\pi R^3} - \beta e^{-\frac{R}{R_c}} + 2\sigma R, \\ \Rightarrow 2\sigma R^4 + R^3(1 - \beta e^{-R/R_c} - e^{\sqrt{\frac{2}{3}}\kappa\phi}) - \frac{2\alpha}{\pi} R_c^3 &= 0. \end{aligned}$$

As  $e^{-R/R_c} \ll 1$  for  $R \gg R_c$ , hence, we may simplify the LHS of above equation to

$$R^4 + R^3 \left( \frac{1 - e^{\sqrt{\frac{2}{3}}\kappa\phi}}{2\sigma} \right) - \frac{\alpha}{\sigma\pi} R_c^3 = 0. \quad (\text{B2})$$

Solving this equation in WolframMathematica we find,

$$R = \frac{1}{8\sigma} \left( -1 + e^{\sqrt{\frac{2}{3}}\kappa\phi} + 4\sigma\sqrt{A - B + C} \right), \quad (\text{B3})$$

where

$$\begin{aligned} A &= \frac{(-1 + e^{\sqrt{\frac{2}{3}}\kappa\phi})^2}{16\sigma^2}, \\ B &= \frac{8\alpha R_c^3}{3^{1/3} \left( -9\pi^2(-1 + e^{\sqrt{\frac{2}{3}}\kappa\phi})^2\alpha R_c^3 + \sqrt{3}\sqrt{\pi^3\alpha^2 R_c^6 \left( 27\pi(-1 + e^{\sqrt{\frac{2}{3}}\kappa\phi})^4 + 4096\alpha\sigma^3 R_c^3 \right)} \right)^{1/3}}, \\ C &= \frac{1}{2 \cdot 3^{2/3}\pi\sigma} \left( -9\pi^2(-1 + e^{\sqrt{\frac{2}{3}}\kappa\phi})^2\alpha R_c^3 + \sqrt{3}\sqrt{\pi^3\alpha^2 R_c^6 \left( 27\pi(-1 + e^{\sqrt{\frac{2}{3}}\kappa\phi})^4 + 4096\alpha\sigma^3 R_c^3 \right)} \right)^{1/3}. \end{aligned}$$

It is seen that the solution (B3) of equation (B2) is a complicated one. To simplify our analysis, we ignore the second part of (B3) as absence of this part does not change  $R$  effectively and then consider the solution as follows:

$$R \approx \frac{e^{\sqrt{\frac{2}{3}}\kappa\phi} - 1}{8\sigma}. \quad (\text{B4})$$

Now,

$$\begin{aligned} Rf_R(R) - f(R) &= R e^{\sqrt{\frac{2}{3}}\kappa\phi} - R + \frac{\alpha R_c}{2} + \beta R_c - \sigma R^2 \\ &= R(e^{\sqrt{\frac{2}{3}}\kappa\phi} - 1) + \frac{\alpha R_c}{2} + \beta R_c - \sigma R^2 \\ &= \frac{\alpha R_c}{2} + \beta R_c + \frac{(e^{\sqrt{\frac{2}{3}}\kappa\phi} - 1)^2}{8\sigma} - \frac{(e^{\sqrt{\frac{2}{3}}\kappa\phi} - 1)^2}{64\sigma} \\ &= \frac{\alpha R_c}{2} + \beta R_c + \frac{7}{64\sigma} (e^{\sqrt{\frac{2}{3}}\kappa\phi} - 1)^2 \\ \Rightarrow \frac{Rf_R(R) - f(R)}{2\kappa^2 f_R^2} &= \frac{R_c}{2\kappa^2 f_R^2} \left[ \frac{\alpha}{2} + \beta + \frac{7}{64\sigma R_c} (e^{\sqrt{\frac{2}{3}}\kappa\phi} - 1)^2 \right]. \\ \frac{V(\phi)}{V_0} &= \left[ \frac{\alpha}{2} + \beta + \frac{7}{64\sigma R_c} (e^{\sqrt{\frac{2}{3}}\kappa\phi} - 1)^2 \right] e^{-2\sqrt{\frac{2}{3}}\kappa\phi}, \end{aligned}$$

where  $V_0 = \frac{R_c}{2\kappa^2}$  is the normalization factor. Further,

$$\begin{aligned} V_{eff} &= V(\phi) - \frac{1}{4} T_\mu^\mu e^{-2\sqrt{\frac{2}{3}}\kappa\phi} \\ \Rightarrow \frac{V_{eff}(\phi)}{V_0} &= \frac{V(\phi)}{V_0} + \frac{1}{4V_0} \rho e^{-2\sqrt{\frac{2}{3}}\kappa\phi} \\ \Rightarrow \frac{V_{eff}(\phi)}{V_0} &= \left[ \frac{\alpha}{2} + \beta + \frac{7}{64\sigma R_c} (e^{\sqrt{\frac{2}{3}}\kappa\phi} - 1)^2 + \frac{\rho\kappa^2}{2R_c} \right] e^{-2\sqrt{\frac{2}{3}}\kappa\phi}. \end{aligned}$$

Computation of  $m_\phi$  after correction:

$$\begin{aligned} m_\phi^2 &= \frac{1}{3f_{RR}(R_0)} \left[ 1 - \frac{R_0 f_{RR}(R_0)}{f_R(R_0)} \right] \\ &= \frac{1}{3} \left[ \frac{1}{\frac{6\alpha R_c^3}{\pi R_0^4} + \frac{\beta}{R_c} e^{-\frac{R_0}{R_c}} + 2\sigma} - \frac{R_0}{1 - \frac{2\alpha R_c^3}{\pi R_0^3} - \beta e^{-\frac{R_0}{R_c}} + 2\sigma R_0} \right] \\ &= \frac{1}{3} \left[ \frac{\pi R_c R_0^4}{6\alpha R_c^4 + \pi\beta R_0^4 e^{-\frac{R_0}{R_c}} + 2\sigma\pi R_c R_0^4} - \frac{\pi R_0^4}{\pi R_0^3 - 2\alpha R_c^3 - \pi\beta R_0^3 e^{-\frac{R_0}{R_c}} + 2\sigma\pi R_0^4} \right] \\ &= \frac{\pi R_c R_0^4}{3(6\alpha R_c^4 + \pi\beta R_0^4 e^{-\frac{R_0}{R_c}} + 2\sigma\pi R_c R_0^4)} \left[ 1 - \frac{6\alpha R_c^4 + \pi\beta R_0^4 e^{-\frac{R_0}{R_c}} + 2\sigma\pi R_c R_0^4}{\pi R_c R_0^3 - 2\alpha R_c^3 - \pi\beta R_c R_0^3 e^{-\frac{R_0}{R_c}} + 2\sigma\pi R_c R_0^4} \right] \\ &= \frac{\pi R_c R_0^4}{3 \times 2\sigma\pi R_c R_0^4 (1 + \frac{3\alpha}{\sigma\pi} \frac{R_c^3}{R_0^4} + \frac{\beta}{2\sigma R_c} e^{-\frac{R_0}{R_c}})} \left[ 1 - \frac{2\sigma\pi R_c R_0^4 [1 + \frac{3\alpha}{\sigma\pi} \frac{R_c^3}{R_0^4} + \frac{\beta}{2\sigma R_c} e^{-\frac{R_0}{R_c}}]}{2\sigma\pi R_c R_0^4 [1 + \frac{1}{2\sigma R_0} - \frac{\alpha}{\pi\sigma} \frac{R_c^3}{R_0^4} - \frac{\beta}{2\sigma R_0} e^{-\frac{R_0}{R_c}}]} \right] \\ &= \frac{1}{6\sigma} \left[ \frac{1}{(1 + \frac{3\alpha}{\sigma\pi} \frac{R_c^3}{R_0^4} + \frac{\beta}{2\sigma R_c} e^{-\frac{R_0}{R_c}})} \right] \left[ 1 - \frac{[1 + \frac{3\alpha}{\sigma\pi} \frac{R_c^3}{R_0^4} + \frac{\beta}{2\sigma R_c} e^{-\frac{R_0}{R_c}}]}{[1 + \frac{1}{2\sigma R_0} - \frac{\alpha}{\pi\sigma} \frac{R_c^3}{R_0^4} - \frac{\beta}{2\sigma R_0} e^{-\frac{R_0}{R_c}}]} \right]. \end{aligned}$$

In a region where  $R_c < R < 1/\sigma$ ,

$$\frac{1}{6\sigma} \approx 166667; \left[ \frac{1}{(1 + \frac{3\alpha}{\sigma\pi} \frac{R_c^3}{R_0^4} + \frac{\beta}{2\sigma R_c} e^{-\frac{R_0}{R_c}})} \right] \approx 1; \text{ and } \left[ 1 - \frac{[1 + \frac{3\alpha}{\sigma\pi} \frac{R_c^3}{R_0^4} + \frac{\beta}{2\sigma R_c} e^{-\frac{R_0}{R_c}}]}{[1 + \frac{1}{2\sigma R_0} - \frac{\alpha}{\pi\sigma} \frac{R_c^3}{R_0^4} - \frac{\beta}{2\sigma R_0} e^{-\frac{R_0}{R_c}}]} \right] \approx 1,$$

So, we may write,

$$m_\phi^2 \approx \frac{1}{6\sigma}.$$

In higher curvature condition  $R > R_c$  and  $R > 1/\sigma$  similar to previous case,

$$\frac{1}{6\sigma} \approx 166667.$$

Further,

$$1 + \frac{3\alpha}{\sigma\pi} \frac{R_c^3}{R_0^4} + \frac{\beta}{2\sigma R_c} e^{-\frac{R_0}{R_c}} \approx 1,$$

In this case we find  $\frac{1}{2\sigma R_0} < 1$  instead of  $\frac{1}{2\sigma R_0} > 1$  in previous case along with two negligible terms

$$\frac{\alpha}{\pi\sigma} \frac{R_c^3}{R_0^4} \text{ and } \frac{\beta}{2\sigma R_0} e^{-\frac{R_0}{R_c}}. \text{ Also, } \left[ 1 - \frac{[1 + \frac{3\alpha}{\sigma\pi} \frac{R_c^3}{R_0^4} + \frac{\beta}{2\sigma R_c} e^{-\frac{R_0}{R_c}}]}{[1 + \frac{1}{2\sigma R_0} - \frac{\alpha}{\pi\sigma} \frac{R_c^3}{R_0^4} - \frac{\beta}{2\sigma R_0} e^{-\frac{R_0}{R_c}}]} \right] \approx 1.$$

This allows us to write the scalaron mass at  $R = R_0$  as

$$m_\phi^2 \approx \frac{1}{6\sigma} \left[ 1 - \left[ 1 + \frac{1}{2\sigma R} \right]^{-1} \right] \approx \frac{1}{6\sigma} \left[ 1 - \frac{2\sigma R}{1 + 2\sigma R} \right] \approx \frac{1}{6\sigma} \left[ \frac{1}{1 + 2\sigma R} \right].$$

- 
- [1] V. C. Rubin and W. K. Ford, *Rotation of the Andromeda Nebula from a Spectroscopic Survey of Emission Regions*, *ApJ* **159**, 379 (1970).
- [2] V. C. Rubin, W. K. Ford and N. Thonnard, *Extended Rotation Curves of High-Luminosity Spiral Galaxies. IV. Systematic Dynamical Properties, Sa→Sc*, *ApJ* **225**, L107 (1978).
- [3] V. C. Rubin, *The Rotation of Spiral Galaxies*, *Science* **220**, 4604 (1983).
- [4] K. Garrett and G. Duda, *Dark Matter: A Primer*, *Adv. Astron.* **2011**, 968283 (2011).
- [5] R. Massey, T. Kitching and J. Richard, *The dark matter of gravitational lensing*, *Rep. Prog. Phys.* **73**, 086901 (2010).
- [6] S. Shankaranarayanan and J. P. Johnson, *Modified theories of Gravity: Why, How and What?*, *Gen. Rel. & Grav.* **54**, 44 (2022).
- [7] M. Milgrom, *A modification of the Newtonian dynamics as a possible alternative to the hidden mass hypothesis*, *ApJ* **270**, 365 (1983).
- [8] T. Harko and F. S. N. Lobo,  *$f(R, L_m)$  gravity*, *Eur. Phys. J. C* **70**, 373 (2010).
- [9] T. Harko, F. S. N. Lobo, S. Nojri, S. D. Odintsov,  *$f(R, T)$  gravity*, *Phys. Rev. D* **84**, 024020 (2011).
- [10] S. Capozziello and M. Francaviglia, *Extended Theories of Gravity and their Cosmological and Astrophysical Applications*, *Gen. Rel. & Grav.* **40**, 357 (2008).
- [11] S. Capozziello and M. De Laurentis, *Extended Theories of Gravity*, *Phys. Rep.* **509**, 167 (2011).
- [12] L. Atayde and N. Frusciante, *Can  $f(Q)$  gravity challenge  $\Lambda$ CDM?*, *Phys. Rev. D* **104**, 064052 (2021).
- [13] Y. Sobouti, *An  $f(R)$  gravitation for galactic environments*, *A&A* **464**, 921 (2007).
- [14] C. G. Böhmer, T. Harko, F. S. N. Lobo, *Dark matter as a geometric effect in  $f(R)$  gravity*, *Astropart. Phys.* **29**, 386 (2008).
- [15] T. Harko, *Galactic rotation curves in modified gravity with non-minimal coupling between matter and geometry*, *Phys. Rev. D* **81**, 084050 (2010).
- [16] L. Á. Gegurgel et al, *Galactic rotation curves in brane world models*, *MNRAS* **415** 3275, (2011).
- [17] R. Zaregonbadi, M. Farhoudi and N. Riazi, *Dark matter from  $f(R, T)$  gravity*, *Phys. Rev. D* **94**, 084052 (2016).
- [18] A. Finch and J. L. Said, *Galactic rotation dynamics in  $f(T)$  gravity*, *Eur. Phys. J. C* **78**, 560 (2018).
- [19] N. Parbin and U. D. Goswami, *Scalarons mimicking Dark Matter in the Hu-Sawicki model of  $f(R)$  gravity*, *Mod. Phys. Lett. A* **36**, 2150265 (2021).
- [20] N. Parbin and U. D. Goswami, *Galactic rotation dynamics in a new  $f(R)$  gravity model*, *Eur. Phys. J. C* **83**, 411 (2023).
- [21] H. Shabani and P. H. R. S. Moraes, *Galaxy rotation curves in the  $f(R, T)$  gravity formalism*, *Phys. Scr.* **98**, 065302 (2023).
- [22] S. Chakraborty, *An alternative  $f(R, T)$  gravity theory and the dark energy problem*, *Gen. Rel. & Grav.* **45**, 2052 (2013).
- [23] S. Capozziello, V. F. Cardone, and A. Troisi, *Dark energy and dark matter as curvature effects*, *JCAP* **0608**, 001, (2006).
- [24] A. Joyce, L. Lombriser and F. Schmidt, *Dark Energy Versus Modified Gravity*, *Ann. Rev. Nucl. & Part. Sci.* **66**, 95 (2016).
- [25] P. J. E. Peebles and B. Ratra, *The cosmological constant and dark energy*, *Rev. Mod. Phys.* **75**, 559 (2002).
- [26] H. A. Buchdahl, *Non-Linear Lagrangians and Cosmological Theory*, *MNRAS* **150**, 1 (1970).
- [27] A. A. Starobinski, *A new type of isotropic cosmological models without singularity*, *Phys. Lett. B* **91**, 99 (1980).
- [28] D. J. Gogoi and U. D. Goswami, *A new  $f(R)$  Gravity Model and properties of Gravitational Waves in it*, *Eur. Phys. J. C* **80**, 1101 (2020).
- [29] W. Hu and I. Sawicki, *Models of  $f(R)$  cosmic acceleration that evade solar system tests*, *Phys. Rev. D* **76**, 064004 (2007).
- [30] F. G. Alvarenga, M. J. S. Houndjo, A. V. Monwanou and J. B. C. Orou, *Testing some  $f(R, T)$  gravity models from energy conditions*, *J. Mod. Phys.*, **4**, 130 (2013).
- [31] G. Mohan and U. D. Goswami, *Galactic rotation curves of spiral galaxies and dark matter in  $f(R, T)$  gravity theory*, *IJGMMP* **21**, 2450082 (2024).
- [32] D. Lovelock, *The Einstein tensor and its generalizations*, *J. Math. Phys.* **12**, 498 (1971).
- [33] S. Nojiri and S. D. Odintsov, *Modified Gauss-Bonnet theory as gravitational alternative for dark energy*, *Phys. Lett. B* **631**, 1 (2005).
- [34] T. Chiba,  *$1/R$  gravity and Scalar-Tensor Gravity*, *Phys. Lett. B* **575**, 1 (2003).
- [35] M. Kunz and D. Sapone, *Dark Energy versus Modified Gravity*, *Phys. Rev. Lett.* **98**, 121301 (2007).
- [36] S. Shahidi and H. R. Sepangi, *Brane worlds and dark matter*, *IJMP D* **20**, 77 (2011).
- [37] A. D. Felice and S. Tsujikawa,  *$f(R)$  theories*, *Liv. Rev. Rel.* **13**, 3 (2010).
- [38] T. Faulkner, M. Tegmark, E. F. Bunn and Y. Mao, *Constraining  $f(R)$  Gravity as a Scalar Tensor Theory*, *Phys. Rev. D* **76**, 063505 (2006).
- [39] T. Tamaki, S. Tsujikawa, *Revisiting chameleon gravity-thin-shells and no-shells with appropriate boundary conditions*, *Phys. Rev. D* **78**, 084028 (2008).
- [40] T. Clifton, P. G. Ferreira, A. Padilla and C. Skordis, *Modified Gravity and Cosmology*, *Phys. Rep.* **1**, 513 (2012).
- [41] A. Joyce, B. Jain, J. Khoury and M. Trodden, *Beyond the Cosmological Standard Model*, *Phys. Rep.* **568**, 1 (2015).
- [42] A. Terukina, et al, *Testing chameleon gravity with the Coma cluster*, *JCAP* **04**, 013 (2014).
- [43] K. Koyama, *Cosmological tests of modified gravity*, *Rep. Prog. Phys.* **79**, 046902 (2016).
- [44] C. Burrage and J. Sakstein, *Tests of Chameleon Gravity*, *Liv. Rev. Rel.* **1**, 21 (2018).
- [45] T. Chiba, T. L. Smith and A. L. Erickcek, *Solar System constraints to general  $f(R)$  gravity*, *Phys. Rev. D* **75**, 124014 (2007).
- [46] J. Khoury and A. Weltman, *Chameleon cosmology*, *Phys. Rev. D* **69**, 044026 (2004).
- [47] J. Khoury and A. Weltman, *Chameleon Fields:Awaiting Surprises for Tests of Gravity in Space*, *Phys. Rev. Lett.* **93**, 17110 (2004).
- [48] J. Khoury, *Chameleon Field Theories*, *Class. Quant. Grav.* **30**, 214004 (2013).
- [49] K. Hinterbichler and J. Khoury, *Symmetron Fields:Screening Long-Range Forces Through Local Symmetry Restoration*, *Phys. Rev. Lett.* **104**, 231301 (2010).
- [50] M. M. Verma and B. K. Yadav, *Observational Role of Dark Matter in  $f(R)$  Models for Structure Formation*, *IJMP: Conf. Ss.* **46**,

- 1860045 (2018).
- [51] T. Katsuragawa and S. Matsuzaki, *Modified Gravity Explains Dark Matter?*, *Phys. Rev. D* **95**, 044040 (2017).
- [52] T. Katsuragawa and S. Matsuzaki, *Cosmic History of Chameleonic Dark Matter in  $F(R)$  Gravity*, *Phys. Rev. D* **97**, 064037 (2018).
- [53] P. Burikham and S. Panpanich, *Effects of Chameleon Scalar Field on rotation curves of the galaxies*, *IJMP D* **21**, 1250041 (2012).
- [54] P. D. Mannheim and J. G. O'Brien, *Fitting galactic rotation curves with conformal gravity and a global quadratic potential*, *Phys. Rev. D* **85**, 124020 (2012).
- [55] Y. Shtanov, *Light scalaron as dark matter*, *Phys. Lett. B* **820**, 136469 (2021).
- [56] A. P. Naik, E. Puchwein, A. C. Davis and C. Arnold, *Imprints of Chameleon  $f(R)$  gravity on Galaxy rotation curves*, *MNRAS* **480**, 5211 (2018).
- [57] Q. Li and L. Modesto, *Galactic Rotation Curves in Conformal Scalar-Tensor Gravity*, *Grav. & Cos.* **26**, 99 (2020).
- [58] J. R. Brownstein and J. W. Moffat, *Galaxy Rotation Curves without Nonbaryonic Dark Matter*, *ApJ* **636**, 721 (2006).
- [59] V. D. Falco and et al., *Exploring departures from Schwarzschild black hole in  $f(R)$  gravity*, *Eur. Phys. J. C* **83**, 6 (2023).
- [60] J. Bora, D. J. Gogoi, U. D. Goswami, *Strange stars in  $f(R)$  gravity Palatini formalism and gravitational wave echoes from them*, *JCAP* **09**, 057 (2022).
- [61] D. J. Gogoi and U. D. Goswami, *Cosmology with a new  $f(R)$  gravity model in Palatini formalism*, *IJMP D* **31**, 2250048 (2022).
- [62] T. P. Sotiriou and V. Faraoni,  *$f(R)$  Theories of Gravity*, *Rev. Mod. Phys.* **82**, 451 (2010).
- [63] B. Li, G. B. Zhao and K. Koyama, *Halos and Voids in  $f(R)$  Gravity*, *MNRAS* **421**, 3481 (2012).
- [64] B. Whitt, *Fourth Order Gravity as General Relativity Plus Matter* *Phys. Lett. B* **145**, 176 (1984).
- [65] J. Velásquez and L. Castañeda, *Equivalence between Scalar-Tensor theories and  $f(R)$ -gravity: From the action to Cosmological Perturbations* *J. Phys. Com.* **4**, 055007 (2020).
- [66] V. Faraoni and S. Nadeau, *The (pseudo)issue of the conformal frame revisited*, *Phys. Rev. D* **75**, 023501 (2007).
- [67] M. P. Dabrowski, J. Garecki, D. B. Blaschke, *Conformal transformations and conformal invariance in gravitation*, *Ann. Phys. (Berlin)* **18**, 13 (2009).
- [68] V. Faraoni and E. Gunzig, *Einstein frame or Jordan frame?* *IJTP* **38**, 217 (1999).
- [69] U. D. Goswami and K. Deka, *Cosmological dynamics of  $f(R)$  gravity scalar degree of freedom in Einstein frame*, *IJMP D*, **22**, 1350083 (2013).
- [70] A. V. Frolov, *A Singularity Problem with  $f(R)$  Dark Energy* *Phys. Rev. Lett.* **101**, 061103 (2008).
- [71] S. Weinberg, *Gravitation and Cosmology Principles and Applications of the General Theory of Relativity*, John Wiley & Sons, New York, (1972).
- [72] A. Zanzi, *Chameleonic Theories: A Short Review*, *Universe* **1(3)**, 446 (2015).
- [73] R. Wald, *General Relativity*, The University of Chicago Press, Chicago and London, pp 77 (1984).
- [74] C. A. Sporea, A. Borowiec and A. Wojnar, *Galaxy Rotation Curves via Conformal Factors*, *Eur. Phys. J. C* **78**, 308 (2018).
- [75] A. Stabile and S. Capozziello, *Self-gravitating systems in Extended Gravity*, *Galaxies*, **2(4)**, 520 (2014).
- [76] S. Capozziello, A. Stabile and A. Troisi, *The Newtonian Limit of  $F(R)$  gravity*, *Phys. Rev. D* **76**, 104019 (2007).
- [77] J. P. Mimoso, F. S. N. Lobo and S. Capozziello, *Extended Theories of Gravity with Generalized Energy Conditions*, *J. Phys: Conf. Ss.* **600**, 012047 (2015).
- [78] A. Wojnar and H. Velten, *Equilibrium and stability of relativistic stars in extended theories of gravity*, *Eur. Phys. J. C* **76**, 697 (2016).
- [79] F. Lelli, S. S. McGaugh and J. M. Schombert, *SPARC: Mass Models for 175 Disk Galaxies with Spitzer Photometry and Accurate Rotation Curves*, *AJ* **152**, 157 (2016).
- [80] G. Bothun, C. Impey and S. McGaugh, *Low-Surface-Brightness Galaxies: Hidden Galaxies Revealed*, *PASP* **109**, 745 (1997).
- [81] W. J. G. de Blok and S. S. McGaugh, *The dark and visible matter content of low surface brightness disc galaxies*, *MNRAS* **290**, 533 (1997).
- [82] W. J. G. de Blok and A. Bosma, *High-resolution rotation curves of low surface brightness galaxies*, *A&A.* **385**, 816 (2002).
- [83] W. J. G. de Blok and S. S. McGaugh, *Does low surface brightness mean low surface density?*, *ApJ* **469**, L89 (1996).
- [84] E. V. Karukes and P. Salucci, *The universal rotation curve of dwarf disk galaxies*, *MNRAS* **465**, 4703 (2017).
- [85] S. S. McGaugh, *The Third Law of Galactic Rotation*, *Galaxies* **2(4)**, 601 (2014).
- [86] I. d. Martino, A. Diaferio and L. Ostorero, *Dynamics of dwarf galaxies in  $f(R)$  gravity*, *MNRAS* **519**, 4424 (2023).
- [87] J. F. Navarro, C. S. Frenk and S. D. M. White, *A Universal Density Profile from Hierarchical Clustering*, *ApJ* **490**, 493 (1997).
- [88] Y. Sofue, *The Mass Distribution and Rotation Curve in the Galaxy*, *Plts, Strs. & Str. Systs.* **985**, (2013).
- [89] W. J. G. de Blok et al., *High-Resolution Rotation Curves and Galaxy Mass Models from THINGS*, *AJ* **136**, 2648 (2008).
- [90] T. Kobayashi and K. Maeda, *Can higher curvature corrections cure the singularity problem in  $f(R)$  gravity?* *Phys. Rev. D* **79**, 024009 (2009).
- [91] S. Nojiri and S. D. Odintsov, *The future evolution and finite-time singularities in  $F(R)$ -gravity unifying the inflation and cosmic acceleration*, *Phys. Rev. D* **78**, 046006 (2008).
- [92] A. Dev et al., *Delicate  $f(R)$  gravity models with disappearing cosmological constant and observational constraints on the model parameters*, *Phys. Rev. D* **78**, 083515 (2008).
- [93] K. Bamba, S. Nojiri and S. D. Odintsov, *Future of the universe in modified gravitational theories: Approaching to the finite-time future singularity*, *JCAP* **045**, 0810 (2008).